FRACTURE ANALYSIS OF WOLFCAMP CORE
FROM THE PURE OIL, RED HILLS UNIT No. 1 WELL
LEA COUNTY, NEW MEXICO

Scott Cooper and John Lorenz
FractureStudies LLC
scott@fracturestudies.com
john@fracturestudies.com
www.fracturestudies.com

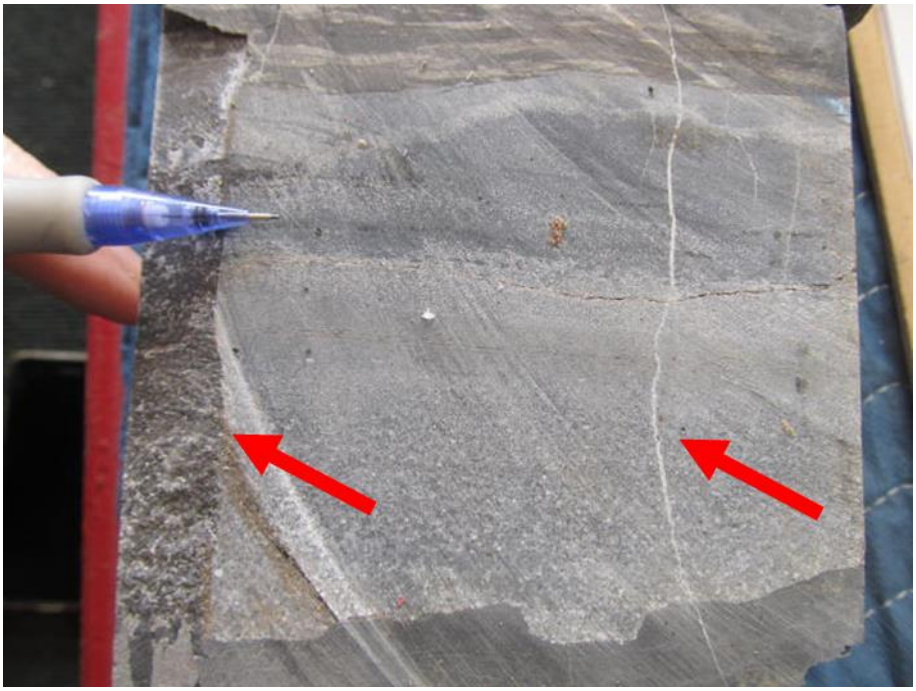

Two calcite-mineralized, high-angle extension fractures cut through a 0.25-ft thick, coarse-grained limestone bed. The fractures extend a short distance into the under- and over-lying black mudstone before narrowing and terminating. The apparent irregularity of the fracture planes is accentuated by the small angle between the fracture planes and the slab face. The rock has broken along the plane of the fracture on the left, exposing the fracture face.

SUMMARY

A well-developed natural-fracture permeability system is documented by 21.4 ft of core cut from deep-marine Wolfcamp strata in the Red Hills Unit No. 1 well, located in southeastern New Mexico in the deep, northeastern part of the Delaware Basin. The sampling of the fracture system captured by the core consists of a population of 50 natural fractures of three types. The numerically-dominant fracture type, which will have a significant impact on reservoir permeability, consists of 42 narrow, strata-bound, incompletely-mineralized vertical extension fractures, which are restricted primarily to limestone beds. Extension fractures strike ENE-WSW, NNE-SSW, and NW-SE, defining three sets, and are very closely spaced. A second fracture type, represented by a single but relatively wide shear fracture in the core, provides important conduits that can connect the fractured limestones across bedding. The more widely spaced shear fractures should tie the extension-fracture system together into an interconnected network of large and small fractures. The third fracture type consists of seven small, occluded, high-angle, ptygmatically-folded extension fractures, which do not contribute to reservoir quality.

Records for this well, drilled in 1963-1964, include the results of a promising drill-stem test and indications of significant lost circulation in the Wolfcamp interval, showing that the natural-fracture network creates significant system permeability despite the low permeability of the matrix rock. The natural-fracture system may be capable of producing at low but commercial rates without the benefit of stimulation, provided that fracture apertures are not damaged by drilling fluids, casing cement, or changes in reservoir pressure during production.

TABLE OF CONTENTS

INTRODUCTION

FractureStudies LLC has logged the fractures found in 21.4 ft of publicly-available core cut from the Permian-age Wolfcamp Formation in the Northern Delaware Basin, southeastern New Mexico, and used the data to assess the natural-fracture and in situ stress system in the reservoir at this location. Although the core is short, it captured a relatively robust fracture dataset that documents a well-developed and pervasive fracture-permeability system. This system is similar to fracture systems found in deeply-buried Wolfcamp strata elsewhere in the basin.

The cored fractures and their analysis presented here illustrate some of the fracture-analysis techniques that can be used to understand and assess fracture permeability systems in unconventional reservoirs. They demonstrate the value of a qualitative understanding of such systems as well as illustrating how to build a quantitative natural-fracture database for use in fracture-controlled fluid-flow models.

The definitions and a description of the methods used in this report are presented in Appendix A. Additional details on fracture interpretations and analysis techniques are provided in two recent textbooks by Lorenz and Cooper (2018, 2020).

CORE DATABASE

The core used for this study comes from the Pure Oil Company Red Hills Unit No. 1 well (API well #30-025-21036, NM Oil Conservation Division well ID #34148, BM 1827). This wildcat well was drilled in Section 32 of T. 25 S., R. 33 E., in Lea County, New Mexico during 1963-1964, and reached a total depth of 21,321 ft, bottoming in a Precambrian diorite. Core from the Wolfcamp section of this well is stored at the New Mexico Bureau of Geology and Mineral Resources, in Socorro, New Mexico, and is accessible to the public. The core was

loaned to FractureStudies LLC through the courtesy of the Bureau and its staff Ron Broadhead, Luke Martin and Annabelle Lopez.

Geographic location of the Red Hills Unit No. 1 well, approximately 40 miles southeast of the town of Carlsbad in southeastern New Mexico, just north of the Texas-New Mexico border.

Wolfcamp core from the Red Hills well was cut from the deep-marine facies of the formation (see Kvale et al., 2020, for a description of Wolfcamp depositional environments), and was cut in the deeper, northeastern part of the Delaware Basin west of the Central Basin Platform. The core was cut between the depths of 13,475-13,499 ft (core depth: well records indicate that the corrected wireline depth is 13,493-13,517 ft). The top of the core is 1,832 ft below the top of the Wolfcamp Formation (picked in the well records at 11,643 ft): assuming that the picked top of the Strawn Formation at 14,310 ft marks the base of the Wolfcamp, the core was cut 835 ft above the base of the formation. This puts it near the top of the bottom third

of the formation. The A, B, C, and D subdivisions of the formation were apparently not yet in use in 1963.

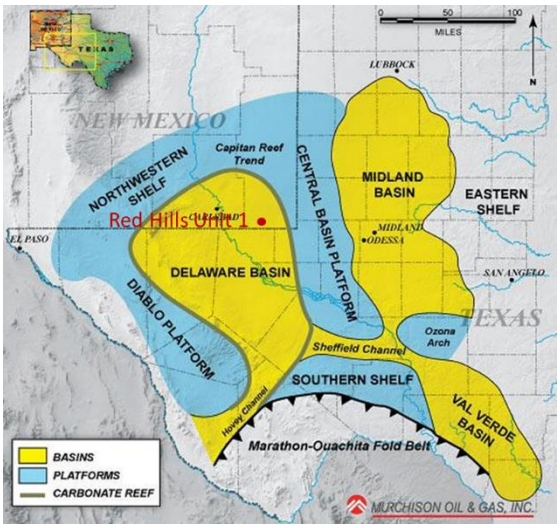

Geologic setting of the Red Hills Unit No. 1 well in the northeastern part of the Delaware Basin, west of the Central Basin Platform, in southeastern New Mexico. Map from https://www.croftsystems.net/oil-gas-blog/the-permian-basin-and-why-it-is-great

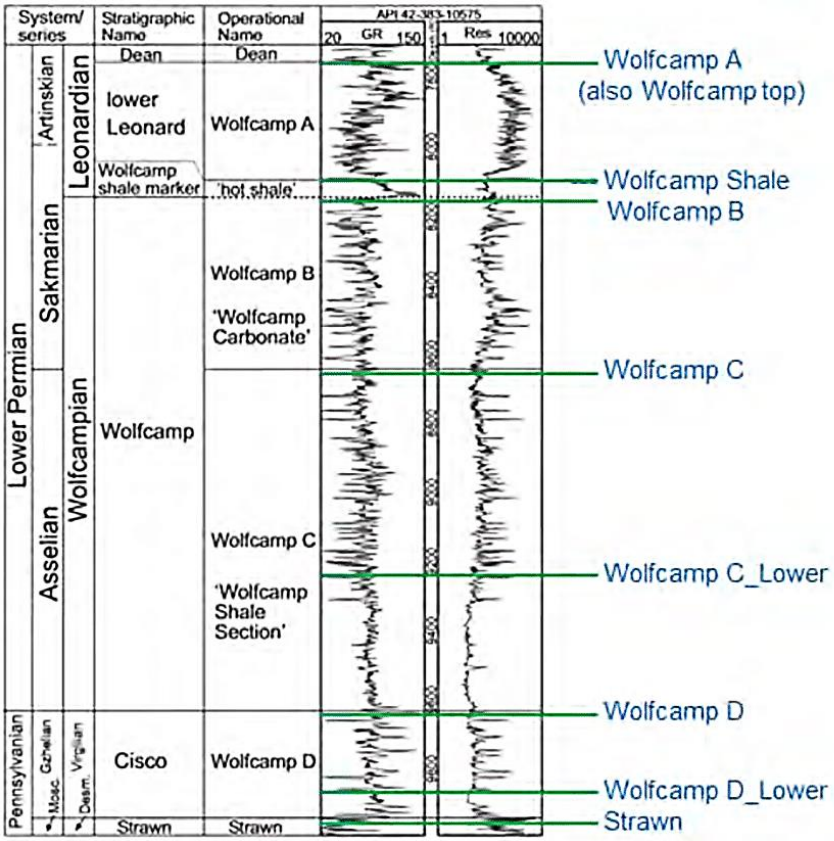

Stratigraphic section of the Wolfcamp Formation in the Delaware Basin (from Thompson et al., 2018). The Red Hills core described here was probably cut from near the middle of the Wolfcamp C interval.

Well records indicate that a nominal 23.4 ft (7.3 m) of Wolfcamp core were cut from the Red Hills Unit No. 1 well. Only 21.4 ft of core remains in the boxes, the missing 2 ft presumably having been removed for sampling although the well files do not document this.

Reported core depth, interval, and core available for the Wolfcamp Formation, Red Hills Unit No. 1 well

Formation/Zone	depth top	depth bottom	cored interval
Wolfcamp Fm	13475.00	13498.40	23.40
Total intervals			23.40
minus samples and drill aheads			2.00
Total			21.40

Reported formation tops in the Red Hills Unit No. 1 well

Formation tops from well log	depth top (ft)
Rustler	874.00
Delaware Sand	4892.00
Cherry Canyon	6174.00
Bone Spring	9020.00
Wolfcamp	11643.00
Strawn	14310.00
Devonian	17424.00
Fussleman	18580.00
Montoya	19000.00
Ellenburger	20898.00
Precambrian Dolerite	21275.00

The logged core is 4½ inches in diameter, somewhat larger than normal. The core has been slabbed, but only the core butts are present in the core boxes stored at the Bureau. Depths are not consistently marked on the butts, so most of the depths used in this report are nominal, being inferred from the three-foot depth intervals marked on the core boxes. The bit-wear pattern at the top of the core confirms that the top of the core was recovered. No similar evidence (core catcher scars, a core stump) is present at the bottom of the core.

The asymmetric, necked core at the top of the core records wobble of the bit before it seated in the bottom of the hole to begin cutting the core.

The Red Hills Wolfcamp core is dominated by black, calcareous, horizontally-laminated mudstones. The mudstones are interbedded with subsidiary units of gray, muddy, fine-grained limestone, and gray, graded, calcarenite limestone. Core condition was fair: the core is relatively complete but many of the core pieces could not be locked together. Some of the core pieces had been inverted in the core boxes, but the up-hole direction of the individual core pieces could often be determined by the orientation of the rainbow arcs of the common induced petal fractures (see Lorenz et al., 1990), and sometimes by reference to the sharp bases and fining-upward graded bedding of the calcarenites.

FRACTURE DATABASE

Natural Fractures

The Wolfcamp core from the Red Hills Unit No. 1 well contains a population of 50 natural fractures, which gives it relatively high averages of 2.34 fractures and 0.53 feet of fracture height per foot of core. Forty-two of these fractures (84%) are vertical to near-vertical, partially-mineralized extension fractures. The rest of the fracture population consists of seven small ptygmatically-folded fractures and one shear fracture. The presence of numerous fractures in this small sampling of the formation indicates that fracturing is pervasive in the reservoir, although the three fracture types do not contribute equally to the reservoir permeability system.

The high-angle extension fractures that dominate the natural-fracture system have vertical to near-vertical dips and are incompletely filled with calcite mineralization. There are several sets of these fractures, with intersecting strikes, thus they provide a significant, relatively high-permeability drainage network within the limestone layers of the reservoir. The cored shear fracture is less well mineralized, and shears should provide significant additional interconnectivity to the fracture network. The seven cored ptygmatically-folded fractures are short, completely mineralized, and isolated: this fracture type does not contribute to reservoir quality.

Fracture intensity summary, all fractures

Fracture type	Analysis	Fractures (#)	Fractures (%)	Sum of fracture height (ft)
extension: high-angle		42	84	10.60
extension: ptygmatic		7	14	0.12
shear: high-angle		1	2	0.65
Total number of fractures	50			
Total feet of fracture height	11.37			
Core interval (ft)	21.40			
Fractures (#)/cored interval (ft)	2.34			
Fracture height (ft)/cored interval (ft)	0.53			

Summary of fracture characteristics, all fractures

Fracture type		Fractures (#)	Height (ft)	Width (mm)	Porosity %	Spacing (mm)	Dip angle (°)
extension: high-angle	Sum		10.60	6.55			
	Count	42	42	42	42	5	42
	Min		0.03	0.05	0	13	80
	Max		1.65	0.40	90	45	90
	Average		0.25	0.16	10.8	33.0	89.4
extension: ptygmatic	Sum		0.12	0.65			
	Count	7	7	7	7		7
	Min		0.01	0.05	0		80
	Max		0.02	0.10	0		90
	Average		0.02	0.09	0.0		87.9
shear: high-angle	Sum		0.65	0.30			
	Count	1	1	1	1		1
	Min		0.65	0.30	40		75
	Max		0.65	0.30	40		75
	Average		0.65	0.30	40.0		75.0

A calcite-mineralized, high-angle extension fracture cuts a coarse-grained calcarenite limestone bed, extending for short distances upward and downward into the adjacent mudstones. Fingertip at the top of the photo for scale.

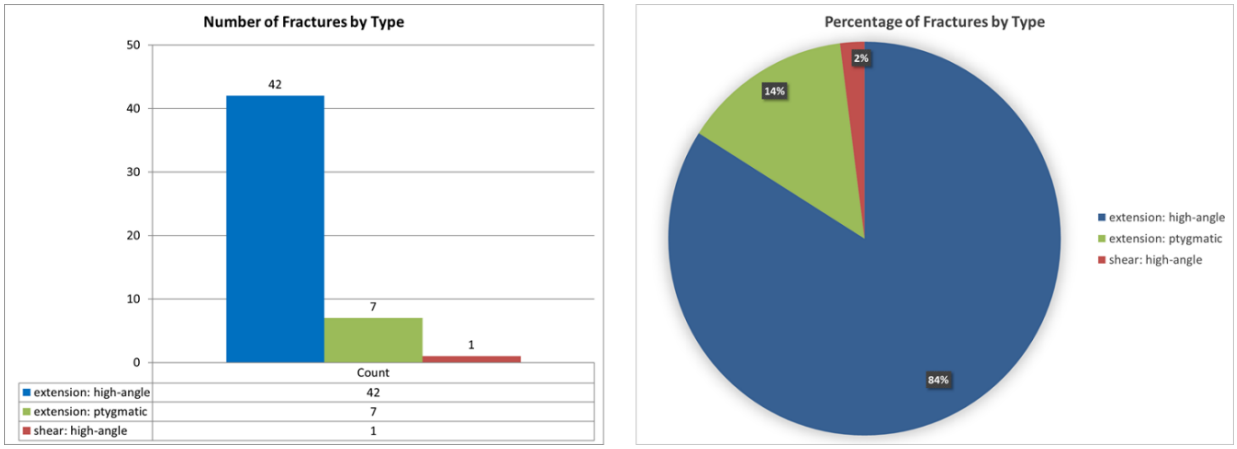

Summary of fracture types by count (left) and percentage (right) (n = 50).

Natural fractures and fracture permeability are irregularly distributed along the 21.4 ft of Wolfcamp core. Two of the three fracture types are preferentially associated with specific lithologies: ptygmatically-folded fractures are restricted to a few mudstone units near the top of the core, whereas the extension fractures are associated with the stiffer, more calcareous beds that are interbedded with the mudstones and present throughout the core. The shear fracture in the core also occurs in a limestone bed. However, it exits the side of the core and it cannot be determined whether it is limited to the limestone, and in fact such shear fractures are unlikely to be restricted to one lithology.

Fractures of all types are mineralized with calcite. However, except for the ptygmatically-folded fractures, there is sufficient remnant void space within the mineralization to significantly enhance system permeability in the fractured beds over that of the matrix.

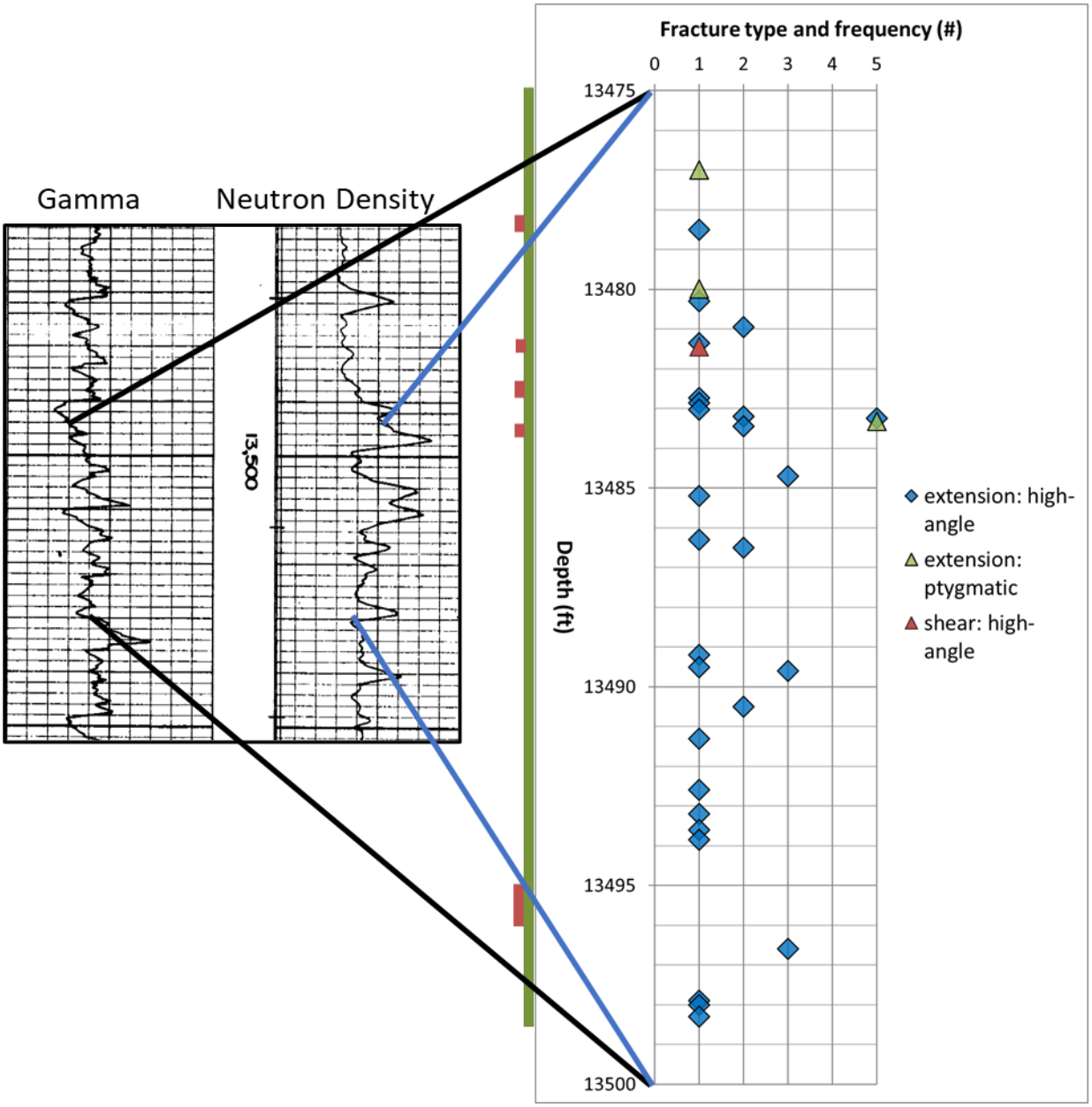

The vertical distribution of all fracture types by depth (n = 50). Overlying data points are darker. Green bar highlights the cored interval, red bars show intervals of missing core. The correlation between core depth and wireline log depth is based on the +18 ft core-depth correction provided by the well records.

Induced Fractures

Petal fractures (Lorenz et al., 1990) are well developed in the Red Hills core. These induced fractures form immediately below the core bit and are captured as the rock below the bit is cored. Petal-fracture cracks in the core often get opened into full breaks during handling and slabbing. Petal fractures angle downward and inward from the outer edge of the core, typically terminating shy of the middle of the core, although they can become extended downward to merge with centerline fractures in some cores. Petals can form as isolated fractures or as a series of parallel, closely-spaced fractures, and they may form on opposing sides of a core or only on one side of the core (for a full description see Lorenz and Cooper, 2018).

This type of induced fracture is not present in the reservoir outside the core and does not contribute to reservoir permeability, consequently the fractures must be distinguished from natural fractures so that they do not get included in the fracture database. However, petal fractures do provide an important orientation reference for nearby natural fractures since they strike parallel to the maximum in situ horizontal compressive stress. These drilling-induced fractures were not individually logged, but the angle between the strikes of natural and petal fractures were recorded.

Two nested, unmineralized, induced petal fractures (dashed black lines are drawn on the core surface adjacent to the petal fractures) in a section of core consisting of gray limestone overlying black mudstone. The fractures do not extend downward into the core any further than shown here. Petal fractures strike parallel to the maximum horizontal compressive stress, thus all petal fractures in a core have nearly parallel strikes and can be used as an orientation reference for natural fractures. Petal-fracture planes always form concave-downward "rainbows" where they intersect the curved core surface, rather than concave-upward "smiles," so they also provide a reference for the uphole direction of a core.

THE NATURAL-FRACTURE SYSTEM IN THE WOLFCAMP FM, RED HILLS CORE

INTRODUCTION

This section provides a detailed characterization of the population of 50 natural fractures logged in the 21.4 ft of Red Hills No. 1 Wolfcamp core. As noted, three types of fractures are present, the 42 high-angle extension fractures comprising the largest sub-population. These fractures not only dominate the fracture system numerically, they should control the reservoir permeability system despite being partially occluded by calcite cement. Since they are closely associated with the limestones, the high-angle extension fractures provide a vertically-limited but laterally-extensive system of fracture-controlled permeability enhancement. These fractures have multiple, intersecting strikes, significantly increasing the lateral interconnectivity and the effectiveness of these fractures within the limestone beds.

A second sub-population consisting of one logged shear fracture is also an important contributor to the permeability system despite the small number captured by the core, since this fracture is relatively wide and less occluded by mineralization than the extension fractures. The presence of one fracture in this short core supports the probable existence of a set of widely spaced shear fractures in the reservoir. Shear fractures can significantly enhance the vertical and lateral interconnectivity of a natural-fracture network since they are less likely to be strata-bound than extension fractures.

In contrast, the third sub-population of seven ptygmatically-folded fractures is insignificant. These fractures are short, scattered, and completely filled with mineralization. They contribute little if anything to the reservoir permeability system.

Each of the three fracture types is described separately in detail below.

HIGH-ANGLE EXTENSION FRACTURES

The 42 high-angle extension fractures in the Red Hills core make up 84% of the total logged fracture population. The extension fractures are narrow and consistently mineralized with calcite, but most are not completely occluded, thus permeability along the remnant apertures of these fractures will be significantly higher than matrix permeability, and this sub-population of fractures dominates the Wolfcamp fracture-permeability system within the limestone beds.

Several of the fracture faces display plume structure, which is diagnostic of an origin in extension; elsewhere the fracture faces are obscured by mineralization or the rock has not split open along a fracture to expose its face. Extension fractures form as parallel sets, thus multiple extension-fracture strikes indicate multiple fracturing events. There are at least three sub-sets of extension fractures with different orientations.

The system of extension fractures is well-developed in the Red Hills core. For the total core length of 21.4 ft, these fractures have an average of 1.96 fractures per foot of core and an average of 0.50 ft of fracture height per foot of core. However, extension fractures are concentrated in the more calcareous units which comprise about 40% of the core length, therefore fracture intensity is significantly higher, approximately double the overall average, within the limestones. Conversely, extension fractures are much less common in the interbedded mudstones, and the fractures that do occur in that lithology are narrower and more completely occluded by calcite. Thus, the effective natural-fracture permeability network is concentrated within the calcareous layers, and it is poorly connected vertically between beds.

The extension fractures are closely spaced, with several examples where the core captured one or more parallel fractures. This indicates that the cored limestone layers that contain no fractures or only one fracture are nevertheless fractured, just on a spacing greater than the 4½ inch core diameter.

High-angle extension fractures: ratios of number of fractures per foot of core (intensity) and fracture height per core height (density)

Fracture type	Analysis	Fractures (#)	Fractures (%)	Sum of fracture height (ft)
extension: high-angle		42	84	10.60
Total number of fractures	42			
Total feet of fracture height	10.60			
Core interval (ft)	21.40			
Fractures (#)/cored interval (ft)	1.96			
Fracture height (ft)/cored interval (ft)	0.50			

High-angle extension-fracture summary chart, listing selected measured properties

Fracture type		Fractures (#)	Height (ft)	Width (mm)	Porosity %	Spacing (mm)	Dip angle (°)
extension: high-angle	**Sum**		10.60	6.55			
	Count	42	42	42	42	5	42
	Min		0.03	0.05	0	13	80
	Max		1.65	0.40	90	45	90
	Average		0.25	0.16	10.8	33.0	89.4

The faces of high-angle fractures are marked by subtle plume structure indicating an origin in extension. Left: an incomplete but definitive plume is present on the fracture face, highlighted by oblique lighting. Right: the core captured all of a small fracture face, and the plume shows the classic upward and downward radiation from a horizontal axis as it propagated left to right. The red bracket shows the vertical extent of the natural fracture. (The inclined surface in the core above the fracture resembles a petal fracture, but rather it is a break created when the missing piece of core spalled from the main section of core, as shown by the upward radiating plume and the lip where it intersects the core surface.)

Dips and Distributions- High-Angle Extension Fractures

Extension fractures in the Red Hills core have dip angles that are parallel or nearly parallel to the core axis, thus, assuming the core is vertical, the fractures have near-vertical dips.

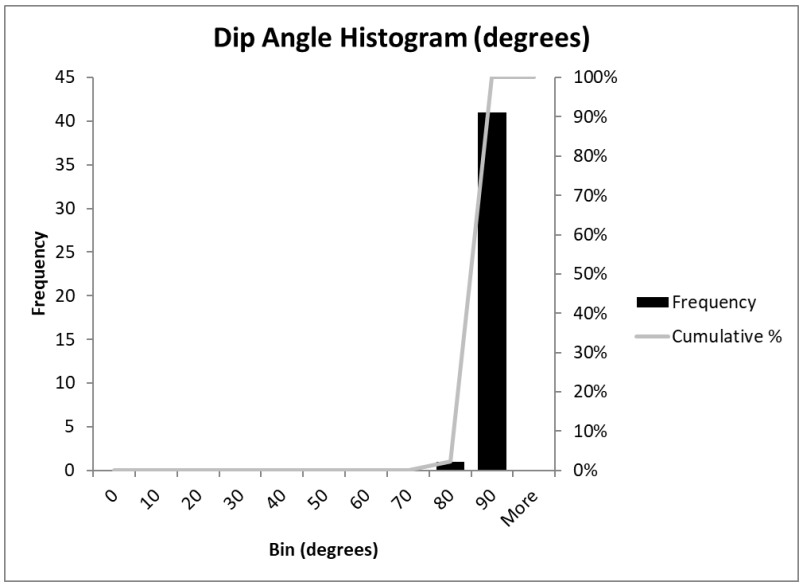

High-angle extension fractures, histogram showing the distribution of fracture dip angles relative to the core axis (n = 42, min 80°, max 90°, ave 89.4°).

Even fractures that appear to have inclined dip angles (left) are in fact nearly vertical: the shallow angle between the fracture plane and the slab face (highlighted by a black dashed line drawn on the end of the core in the photo on the right) accentuates the apparent dip angle of a fracture that is only a few degrees off vertical.

Fracture distribution along the core is primarily controlled by lithology. Most of the 42 extension fractures originated within, and are associated with, the calcarenite limestones and the denser amorphous limestones. However, many fractures extend a short distance from a limestone into an adjacent mudstone. Most of the permeability enhancement related to extension fractures is therefore confined to the relatively brittle, more calcareous lithologies, and the concentrations of fractures in certain zones in the depth-distribution charts reflect lithology. Some of the distribution irregularity however is an artifact of the relatively small sample of the reservoir provided by core: a larger-diameter sampling would show a more uniform fracture distribution in the limestones.

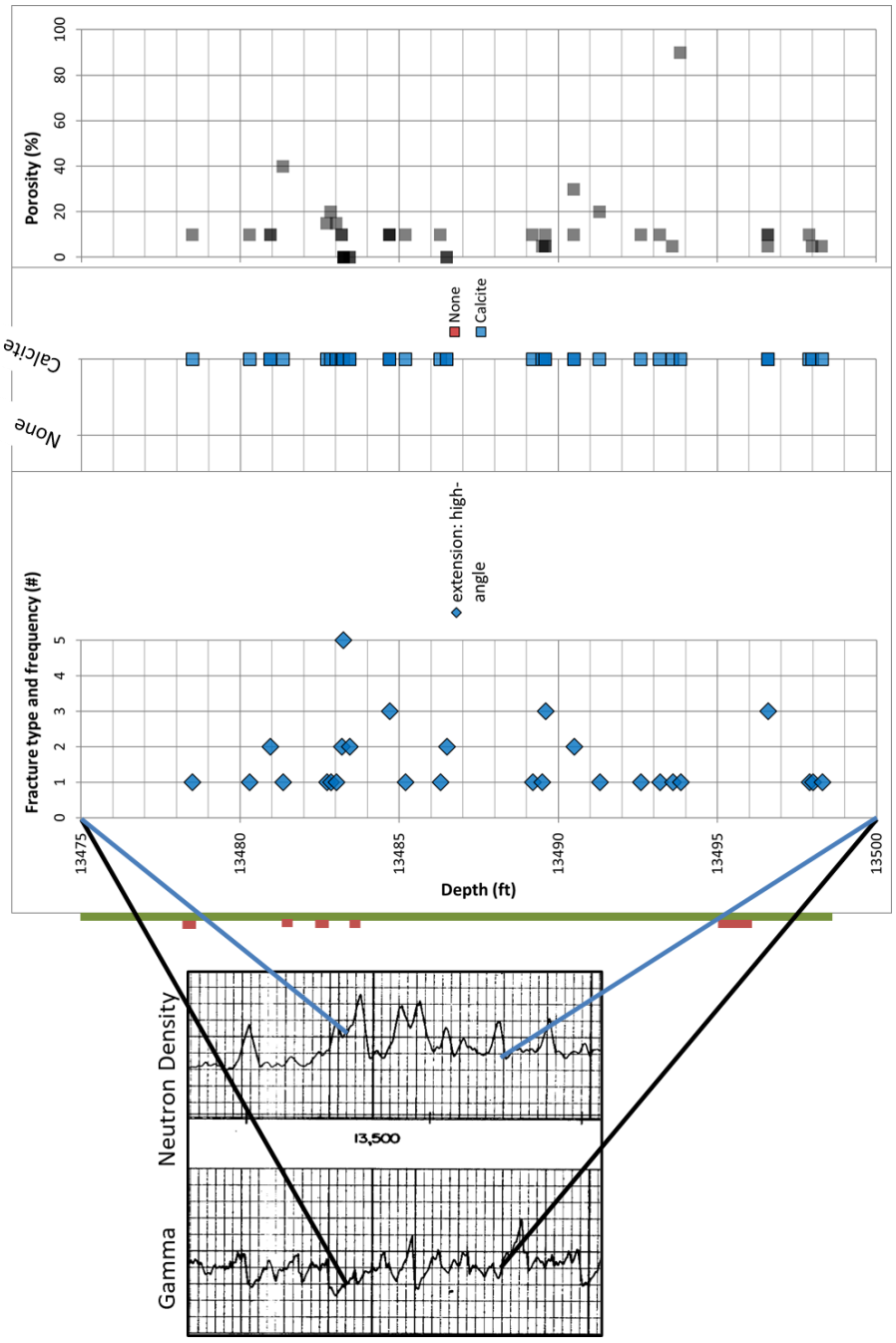

Vertical distribution of extension fractures, fracture-fill components, and average remnant facture porosities (n = 42). The correlation between core depth and the wireline log depth is based on the +18 ft core depth correction provided by the well records.

We identified three basic lithologies in the Red Hills core: a black, variably-calcareous mudstone, and two types of limestone: a gray, fine-grained, amorphous limestone, and a gray, coarse-grained calcarenite limestone. The contacts between these three categories are commonly

gradational rather than distinct, but they serve to show the strong mechanical control lithology had on fracturing. The two limestone types have similar mechanical properties and therefore had similar fracturing responses to stress, and they contain fracture systems with the same characteristics even though they are sedimentologically distinct. In contrast, the interbedded mudstones had a more ductal response to strain and therefore contain significantly fewer extension fractures.

For this analysis, we have combined the two limestone categories since they host the same fracture facies. However, some fractures are hosted by intervals of thinly-interbedded mudstone and limestone, cutting indiscriminately across bedding planes in these heterogeneous zones. Because of this, and because some fractures extend a short distance from their host lithology into an adjacent bed of different lithology, we have plotted fractures vs. lithology in terms of the rock type that hosts at least half and usually greater than 80% of the fracture height.

Over half of the extension fractures are hosted by limestones, and another third of the population occurs in the thinly interbedded facies. Only 17% of the extension fractures are hosted by mudstones even though approximately 60% of the core length consists of mudstone. The limestones and the interbedded facies, comprising about 40% of the core but containing over two-thirds of the extension fractures, together have nearly 5 times the fracture intensity of the mudstones.

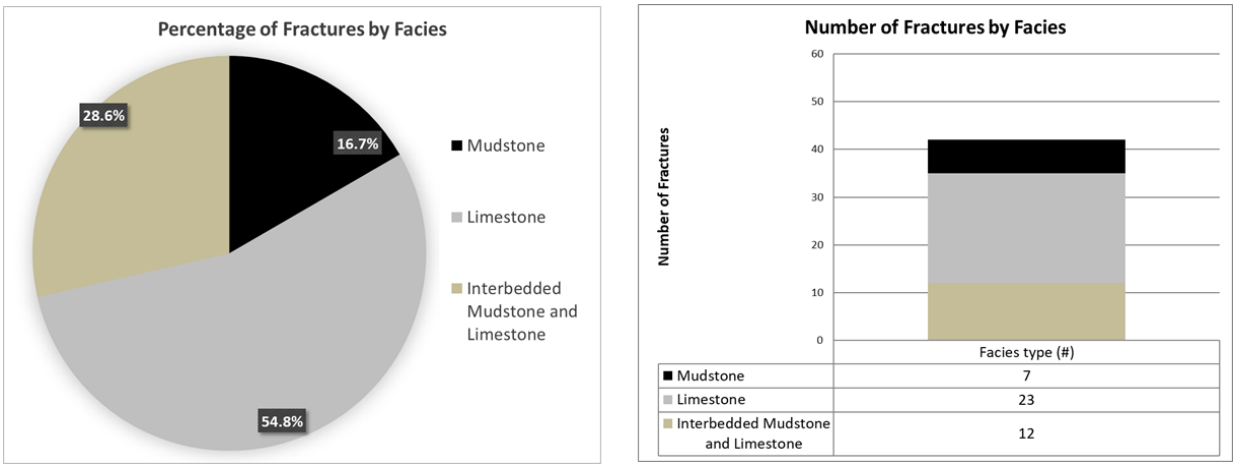

High-angle extension fractures related to the lithologic facies that contains the majority of their height (n = 42). Percentages of fractures within facies: mudstone (16.7%), limestone (54.8%), interbedded mudstone and limestone (28.6%).

High-angle extension fractures that cut across heterogeneous units of interbedded limestones and mudstones. Left; a wide, tall fracture (arrow points to the fracture plane, which is nearly parallel to the slab face) that is at least 0.7 ft tall. Right; several fractures in a heterogeneous lithology, the tallest of which, highlighted by a dotted black line drawn adjacent to the fracture, cuts across multiple thin beds of limestone and mudstone. Shorter fractures, highlighted by pencil lines drawn adjacent to the fractures, are strata-bound within the thin limestone units.

Heights and Terminations: High-Angle Extension Fractures

The average vertical extension fracture is relatively short, only 0.25 ft tall, but in part these are truncated measurements because for some fractures the full height is not present in the core and only a partial height could be measured. Measurable fracture heights are as much as 1.65 ft, indicating that the spectrum of extension fractures includes significant fracture heights.

A cross plot comparing fracture height to the thickness of that fracture's host bed shows that lithology is a strong control on fracture height, even though many of the fractures are slightly taller than the thickness of the primary host bed. Taller and shorter fracture heights are not concentrated in any particular part of the core, in part a function of the incomplete dataset and in part related to the distribution of bedding thicknesses, but fracture height that is commensurate with bed thickness is the general rule.

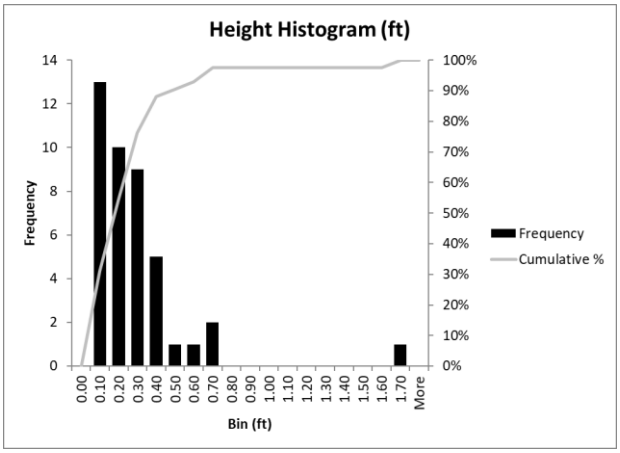

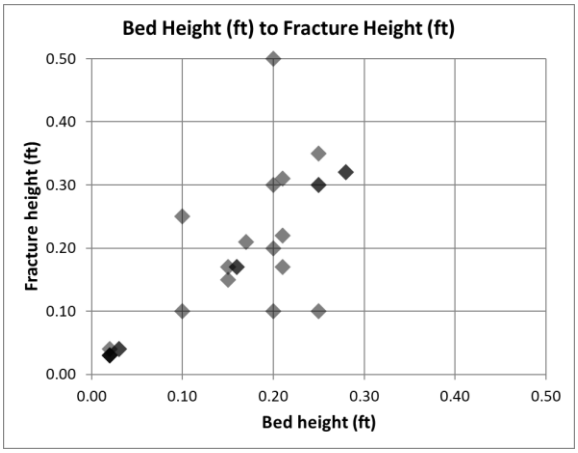

Left: high-angle extension fracture height histogram (n = 42; min 0.03, max 1.65, ave 0.25 ft). Right: high-angle extension bed thickness to fracture height cross plot (n = 27). The high-angle extension fractures have a range of heights that is largely controlled by the thickness of the host bed. Some of the shorter fractures, falling to the right of the 1:1 line on this plot, are incomplete fractures where the full fracture height could not be measured in the existing core (see the next figure). Darker points highlight overlapping data.

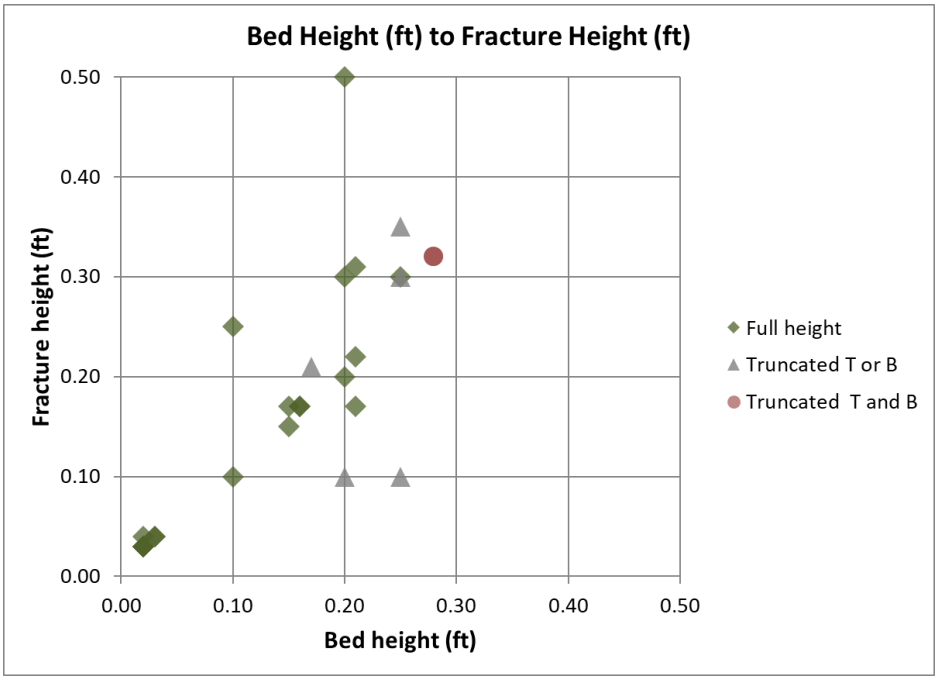

High-angle extension fractures; cross plot of bed thickness and fracture height, showing fracture truncation type (n = 27). Truncated fractures are less likely to extend for the full thickness of a bed, but in the case of the Red Hill core, even the truncated fracture heights are typically equal to or greater than bed thickness since the full fracture heights are commonly slightly taller than bed thickness.

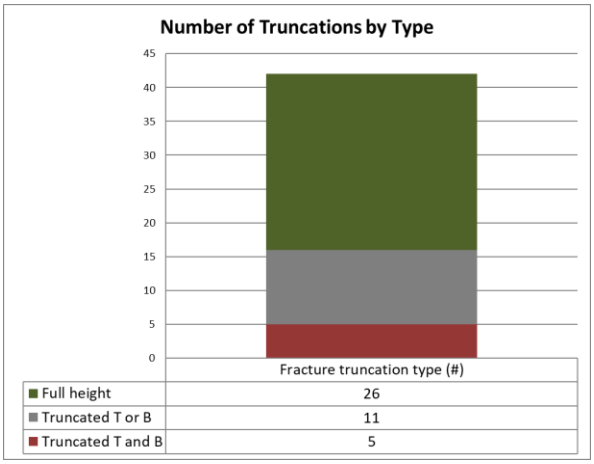

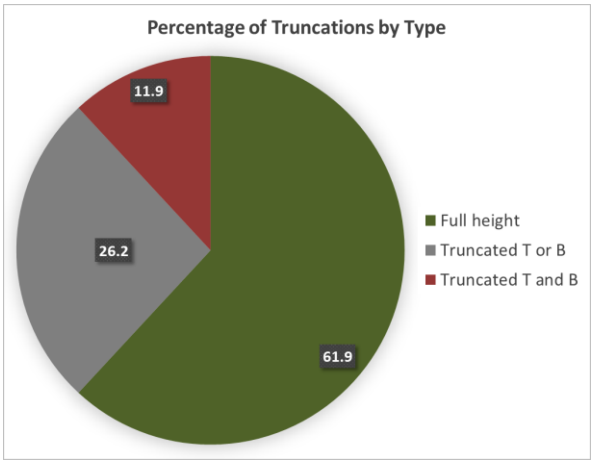

High-angle extension fracture truncation-type charts (n = 42). Truncation type percentages: full height (61.9%), truncated Top (T) or Base (B): 26.2%. Truncated T and B: 11.9%. The top and bottom terminations of most of the cored extension fractures can be found in the core, indicating that the fracture-height data are robust.

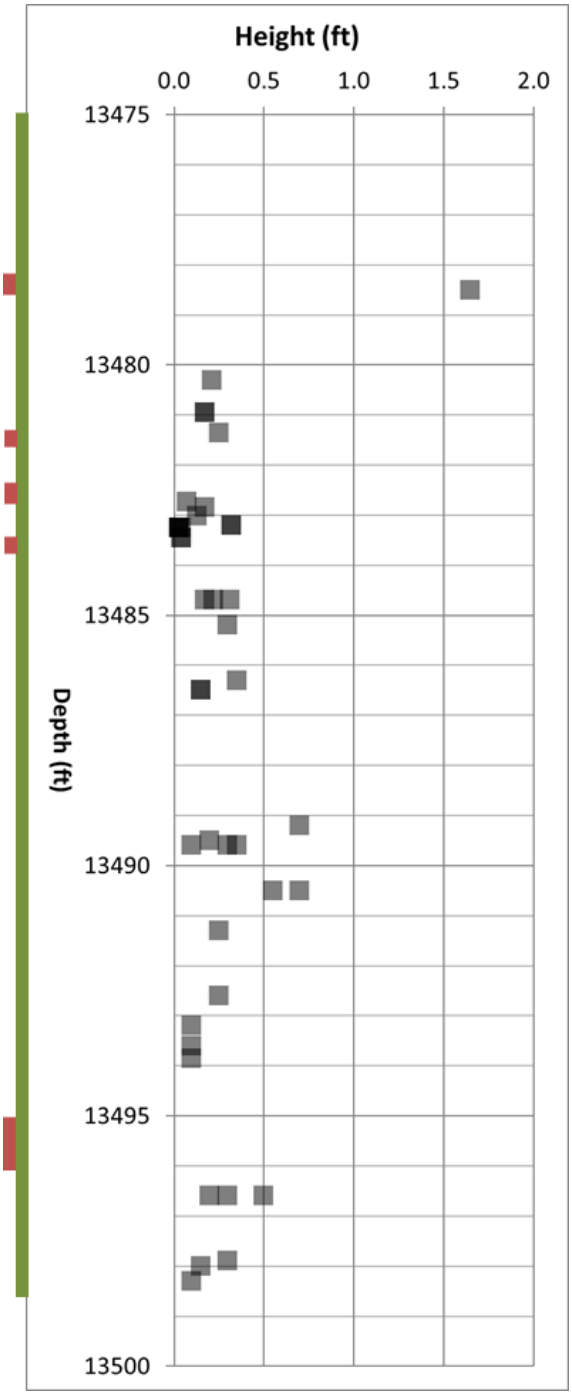

High-angle extension fractures; distribution of heights by depth (n = 42).

High-angle extension fractures in the Red Hills core have several vertical-termination types (each fracture has an upper and a lower termination, therefore the number of terminations is twice the number of fractures). They may terminate at the contact between two contrasting lithologies (at a Lithology change, or "AL" in the database tables), they may terminate blindly for no apparent reason within the host lithology (within a Lithology, "IL"), they may extend from the main host lithology into the adjacent lithology for a short distance before narrowing and terminating (out of lithology, or "OL"). There are also two types of unconstrained terminations, out of core ("OC"), where the fracture exits the side of the core before terminating, and unknown ("Unk"), where the fracture termination has been lost in a missing sample or rubble zone.

Slightly over half (54.8%) of the logged vertical terminations are "out of lithology," reflecting the propagation of the extension fractures for short distances out of a host limestone lithology and into an adjacent mudstone, probably due to a minimal contrast in mechanical properties between the two lithologies at the time of fracturing. This is supported by the observed propagation of fractures across the heterogeneous units, as noted above. The fact that there were, nevertheless, mechanical differences however minor between the units is shown by the 19% of the fractures that terminated at lithologic boundaries. Only one fracture tip failed to propagate either to or beyond a bedding contact, terminating blindly within a homogeneous lithology. The remaining 25% of the vertical fracture terminations are unknown or out of the core.

In other Wolfcamp cores we have logged, one subset of high-angle extension fractures is confined to limestones, another to the mudstones, and a third extends across all units regardless of lithology. Three fracture sets in the Red Hills core are also distinguished by strike, and it is possible, even probable, that the three fracture types have affinities to different lithologies although this cannot be proven with the limited data available from this short core.

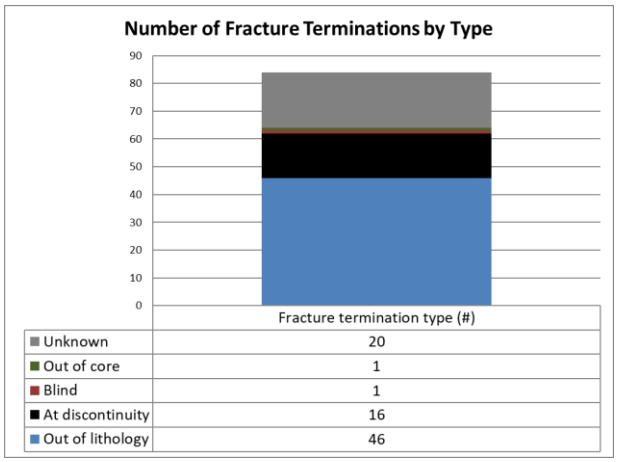

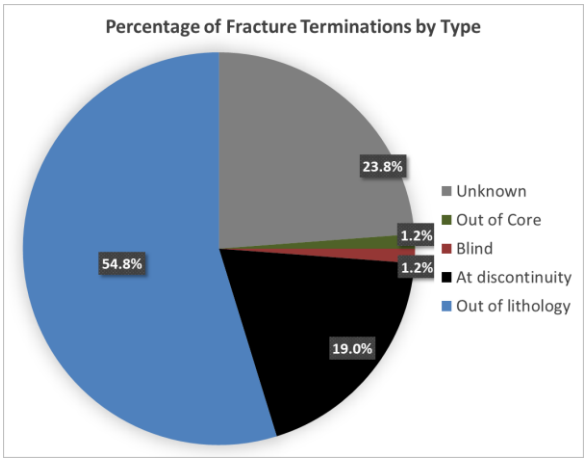

High-angle extension fracture termination charts (n = 84). Termination type percentages: unknown (23.8%), out of core (1.2%), blind (1.2%), at discontinuity (19.0%), out of lithology (54.8%).

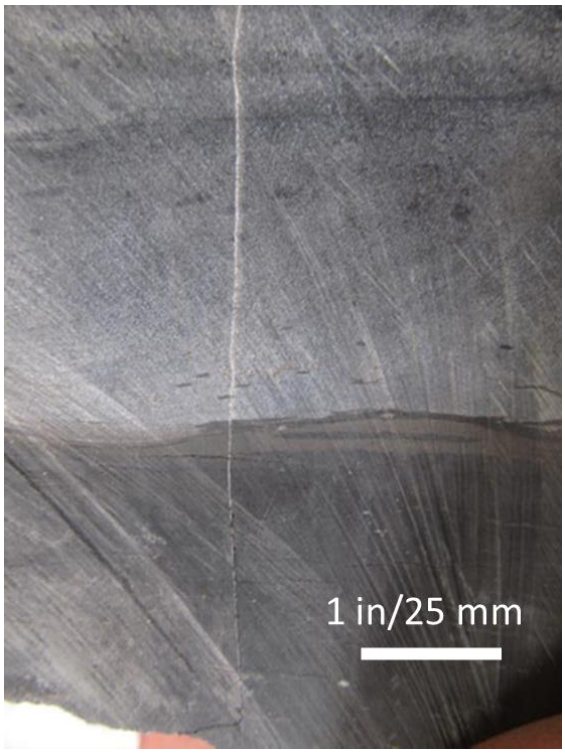

A vertical, calcite-mineralized extension fracture in a gray limestone narrows as it extends downward into the underlying black mudstone before terminating. About 80% of the fracture height occurs in the limestone, but it is taller than the bed thickness and therefore not in the strictest sense "strata-bound." It is, however, effectively strata-bound in that it does not connect vertically across mudstones to connect with fracture systems in limestones higher or lower in the formation.

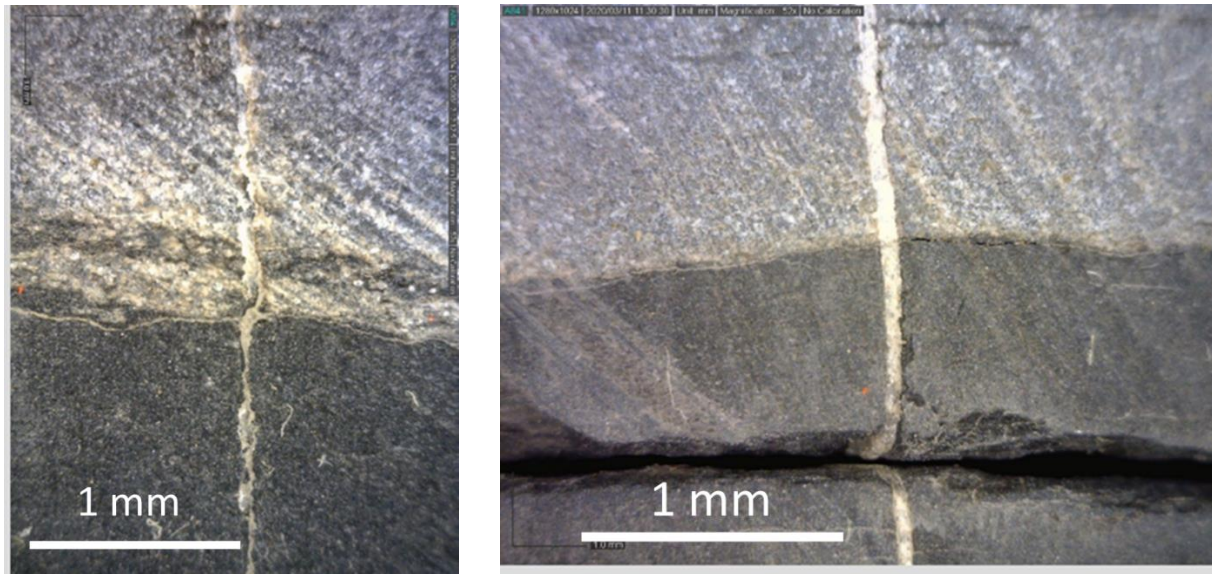

Close-up photos showing calcite-mineralized fractures that extend across lithologic boundaries and into the adjacent mudstones.

Widths, Apertures, and Mineralization: High-Angle Extension Fractures

The high-angle extension fractures in the Red Hills core are all filled to some degree with calcite mineralization. Incomplete mineralization is obvious in the widest fractures, evidenced by euhedral calcite crystal faces that document the presence of open void space along the fracture plane at the time of mineralization. Elsewhere, particularly with the narrower fractures, the remnant fracture aperture within the mineralization is less apparent but can be demonstrated by the slower rate of water evaporation from the fracture slots than from the adjacent matrix.

The average fracture width is only 0.16 mm but the range is up to 0.4 mm. Within those fracture widths, the average remnant porosity is only 10.8%, but the range is up to 90%. The wider fractures typically have greater remnant fracture porosity, i.e., they are less fully occluded by calcite. Similarly, the wider fractures are also commonly the taller fractures. The wider, taller, less-occluded fractures should dominate the Wolfcamp fracture-permeability system, and although only a few were cored, it must be remembered that a core is a very small sampling of a reservoir, and that the presence of any such fractures in a short core indicates that they are well developed and common, even numerous, in the reservoir. No locations along the short Red Hills core show preferential development of fracture width, mineralization, or remnant fracture aperture.

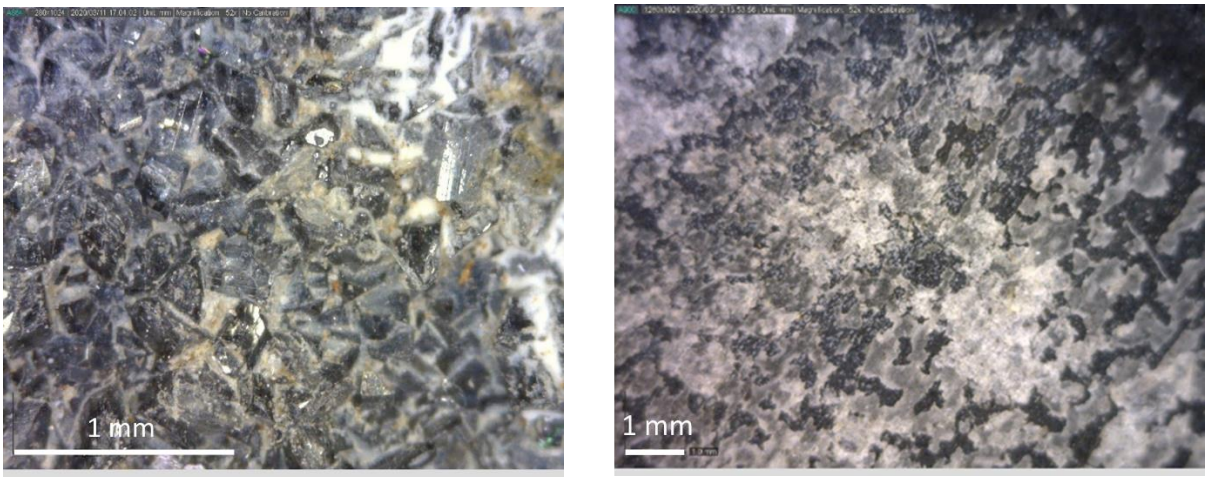

Two photomicrographs of fracture-face mineralization. Left: crystalline calcite on this fracture face in a limestone indicates the presence of significant void space between the fracture walls despite mineralization. Right: a non-crystalline, flaky calcite layer coats the face of a much narrower fracture in a mudstone. The dark patches showing through the mineralization are the host-rock wall that is exposed where the calcite has peeled off the fracture face. This fracture aperture is completely occluded by calcite.

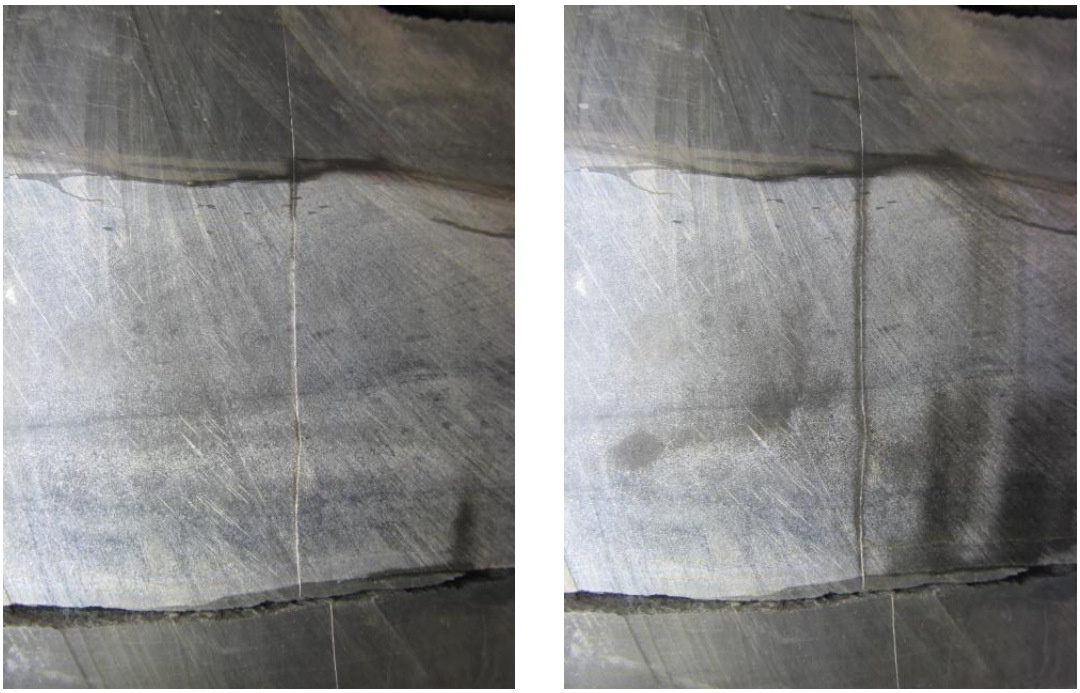

Two views of a calcite-mineralized fracture as exposed on the slab face of the core. Left: the dry core. Right: a view of the same face after it has been wetted and starts to dry--the fracture plane dries more slowly since the remnant porosity within the fracture mineralization wicks water, staying wet longer than the low-porosity limestone.

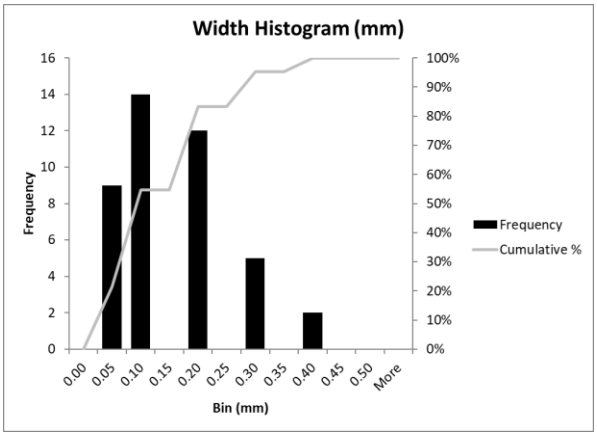

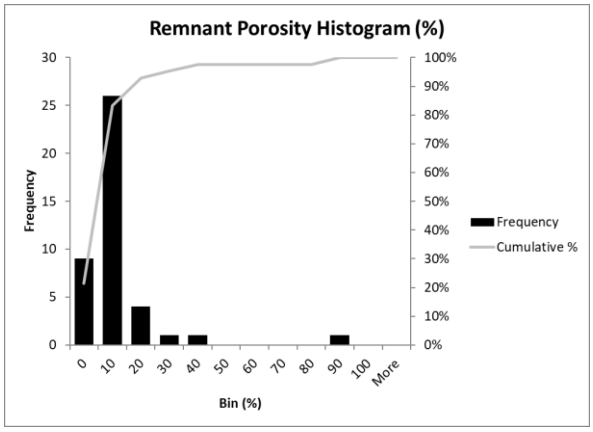

Left: high-angle extension fracture width histogram (n = 42; min 0.05, max 0.40, ave 0.16 mm). Right: high-angle extension remnant fracture porosity histogram (n = 42; min 0%, max 90%, ave 10.8%). The distributions of both fracture widths and remnant fracture porosities are log-normal, which is typical of many extension-fracture characteristics including heights, widths, spacings, and lengths.

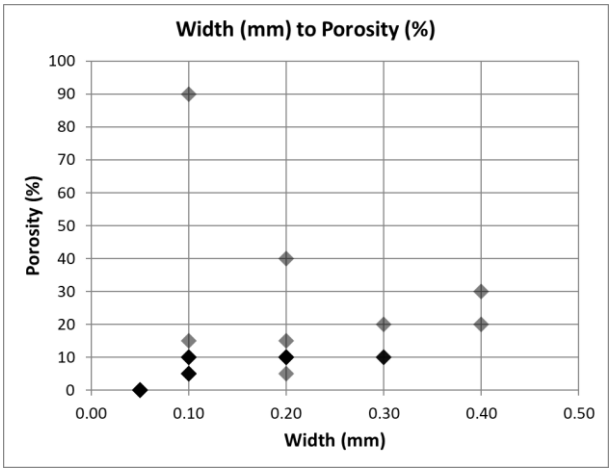

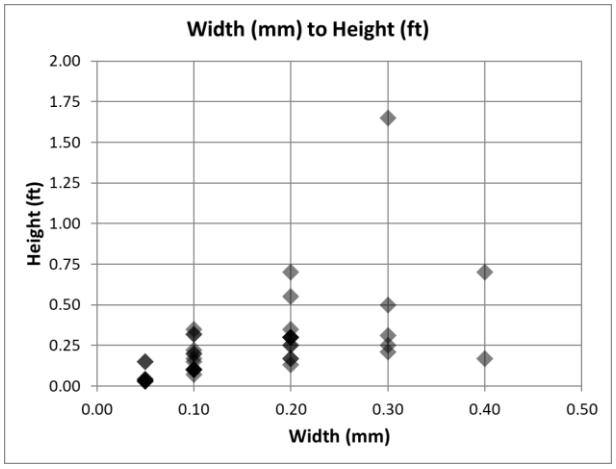

Left: high-angle extension fractures, width to fracture porosity cross plot (n = 42), showing that wider fractures are generally less fully occluded than narrower fractures. Right: high-angle extension fracture width to fracture height cross plot (n = 42), showing that taller fractures tend to be wider. Darker points highlight overlapping data.

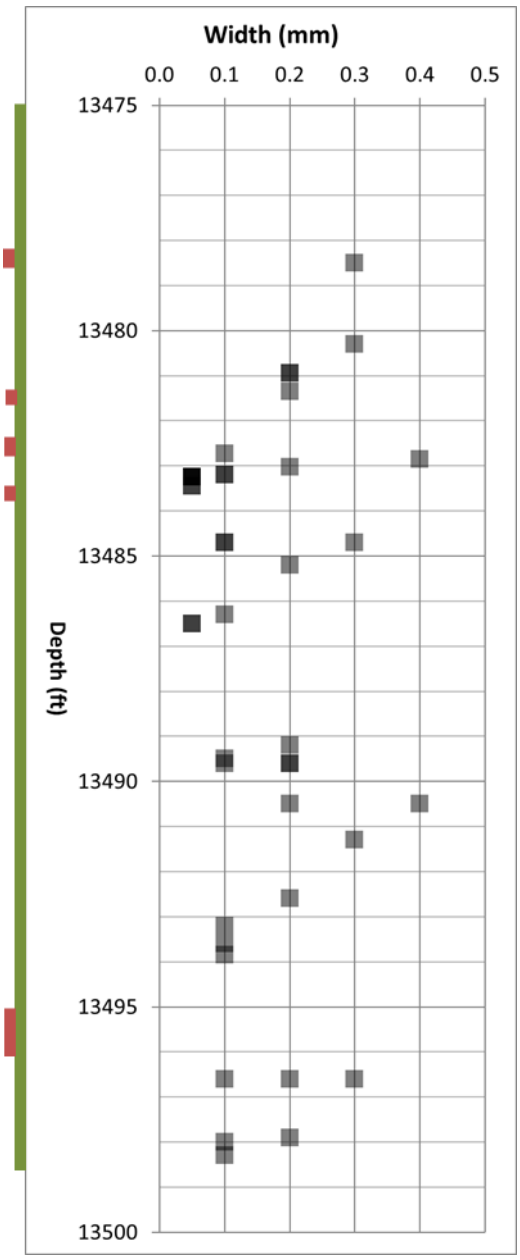

Vertical distribution of the widths of high-angle extension fractures (n = 42). Overlying data points are darker.

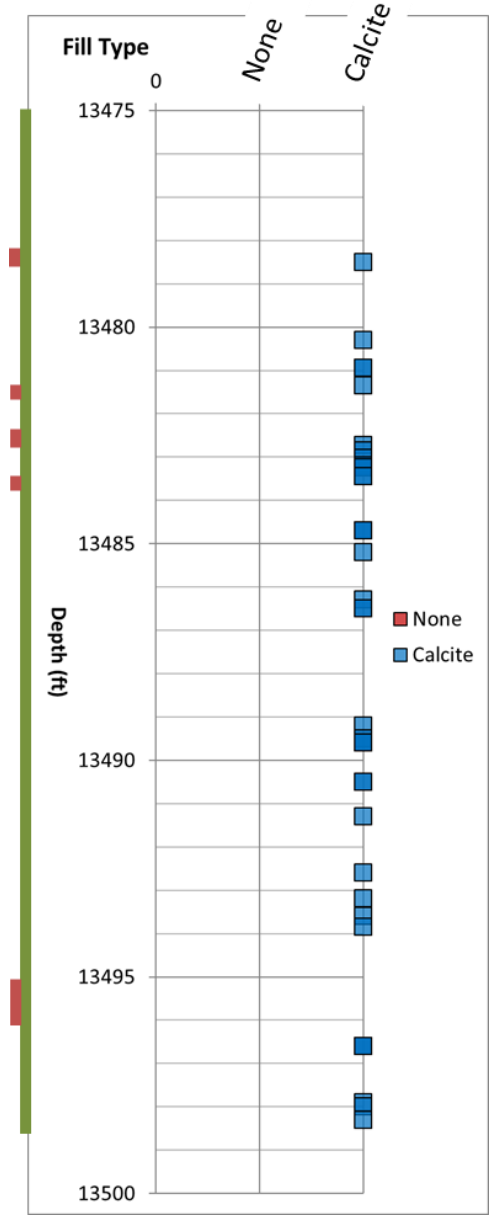

Vertical distribution of the high-angle extension fracture filling components (n = 42). Overlying data points are darker.

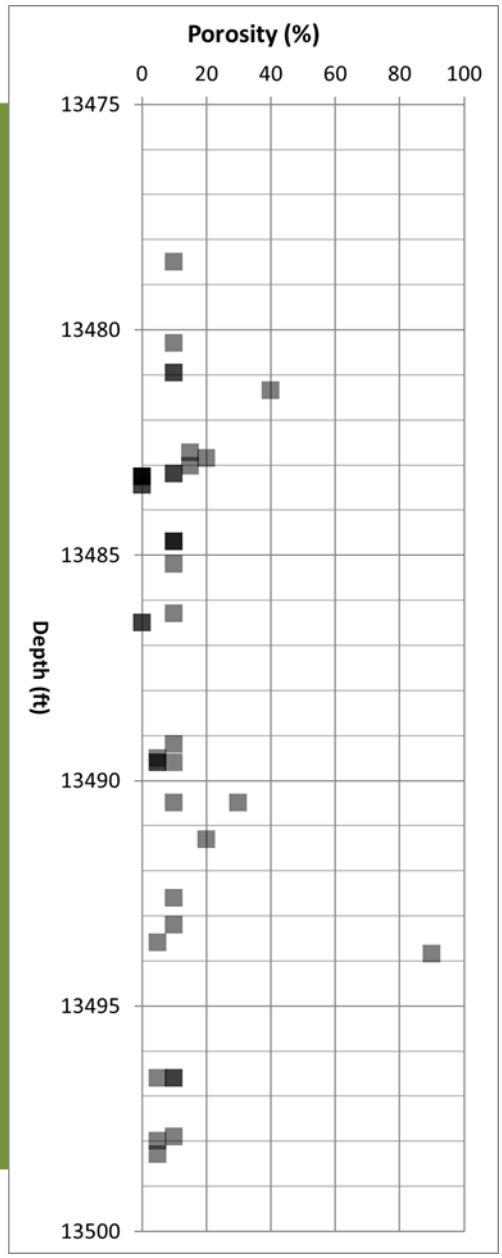

Vertical distribution of the remnant fracture porosity within partially-mineralized high-angle extension fractures (n = 42; min 0%, max 90%, ave 10.8%).

Spacings: High-Angle Extension Fractures

The spacings of five pairs of adjacent, parallel, high-angle extension fractures were captured by the vertical, 4½ inch (11.4 cm) diameter core. The fact that any pairs of parallel fractures of the same set were captured in single pieces of core indicates that the spacing of the extension fractures is quite small. These spacings were measured wherever possible since they record the lower end of a range of spacings in the reservoir. They can be extrapolated qualitatively to estimate that the full range of spacings extends up to one or two feet, and to infer that the extension fractures are generally quite closely spaced.

The core diameter limits the maximum spacing that can be captured, so the average measurable spacing of 33 mm (ranging from 13 mm to 45 mm) represents the lower end of a spectrum of fracture spacings that are probably log-normally distributed. Moreover, the fracture population probably follows the typical extension-fracture pattern where larger fractures are more widely spaced and a myriad of smaller fractures typically occur closer together. This distribution is also suggested by the cross plot showing that the taller fractures tend to have wider spacings.

The apparent clustering of measurable spacings in the upper third of the core is probably created by the small dataset, and by the small sampling of the reservoir provided by core.

Measurable spacings (red arrows) between two pairs of narrow, closely-spaced, calcite-mineralized high-angle extension fractures (highlighted by dashed black lines drawn adjacent to the fractures), exposed on a bedding plane.

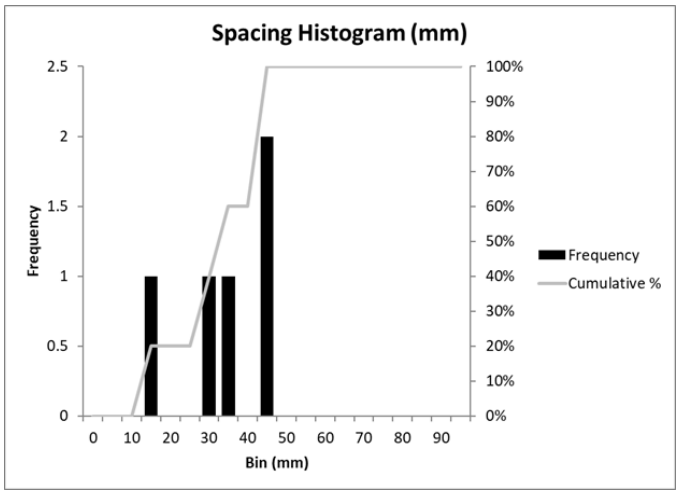

High-angle extension-fracture spacing histogram (n = 5; min 13, max 45, ave 33.0 mm).

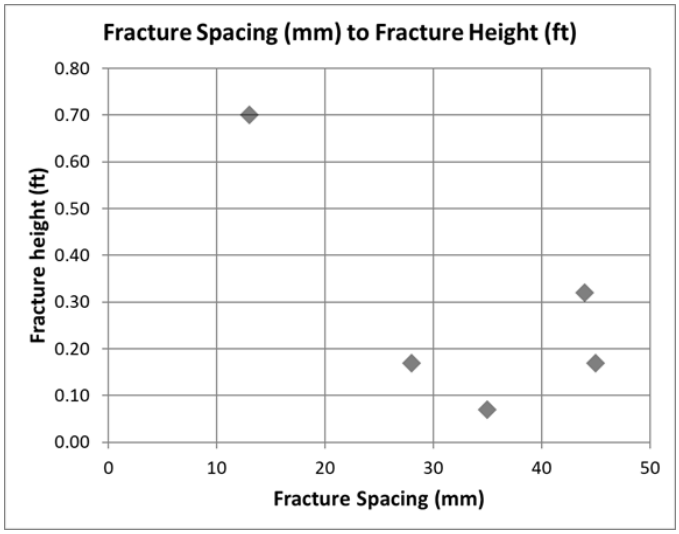

High-angle extension fractures, fracture spacing to fracture height cross plot (n = 5). Except for one pair of closely-spaced relatively tall fractures, the taller fractures are more widely spaced.

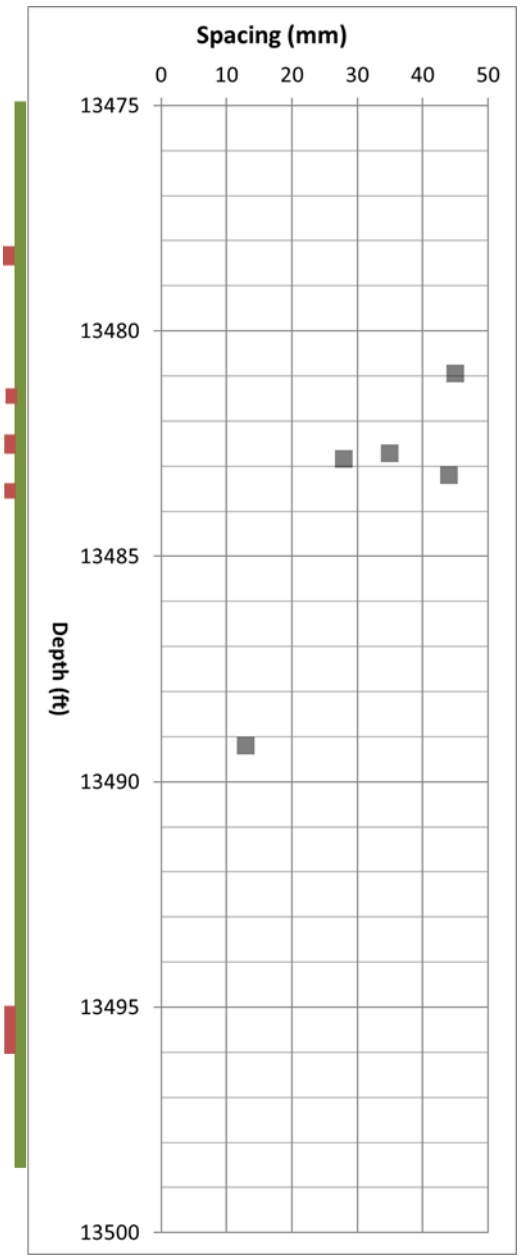

High-angle extension fractures, measured fracture spacings by depth (n = 5).

Strikes: High-Angle Extension Fractures

Two types of fracture strike data can be obtained from the un-oriented Red Hills core: 1) measurements of fracture strikes relative to other natural fractures, and 2) measurements of strikes relative to the orientation reference provided by coring-induced petal fractures. The two methods give consistent results, indicating that there are three fracture sets with three unique strikes in the Wolfcamp reservoir. Moreover, since petal fracture strikes are controlled by the in situ stresses, a good estimate of absolute fracture strikes relative to north can be made by rotating the rose plot of strikes relative to petal fractures so that the petal fractures are aligned with the reported ENE-WSW trending local maximum horizontal compressive in situ stress. Using these methods, the Red Hills fracture-strike data suggest that the three fracture sets strike approximately ENE-WSW, NNE-SSW, and NW-SE. The fractures of the three sets appear to be uniformly developed vertically along the core.

The fracture dataset is not large enough to determine the relative ages of the fracture sets from abutting relationships, nor is it large enough to determine whether the fractures of one set might be more effective (i.e., taller, wider, more intensely developed, or less completely mineralized) than the other sets. These important determinations could probably be made using data from a longer, more intact vertical core, and/or from a horizontal core.

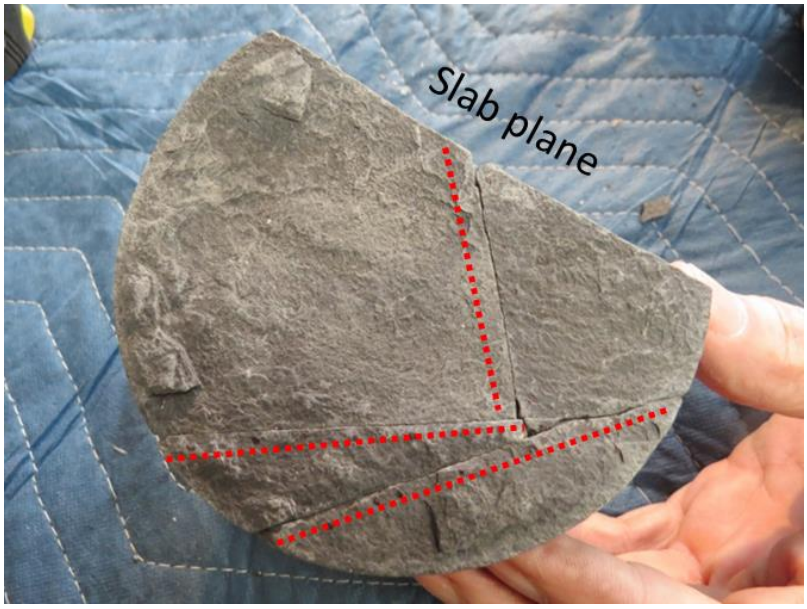

Looking down-hole at three fracture planes with intersecting strikes. The intersection angles between these fractures can be measured directly. More commonly the fractures occur in different pieces of core that cannot be locked together, so the relative natural-fracture strikes must be determined by reference to petal-fracture strikes.

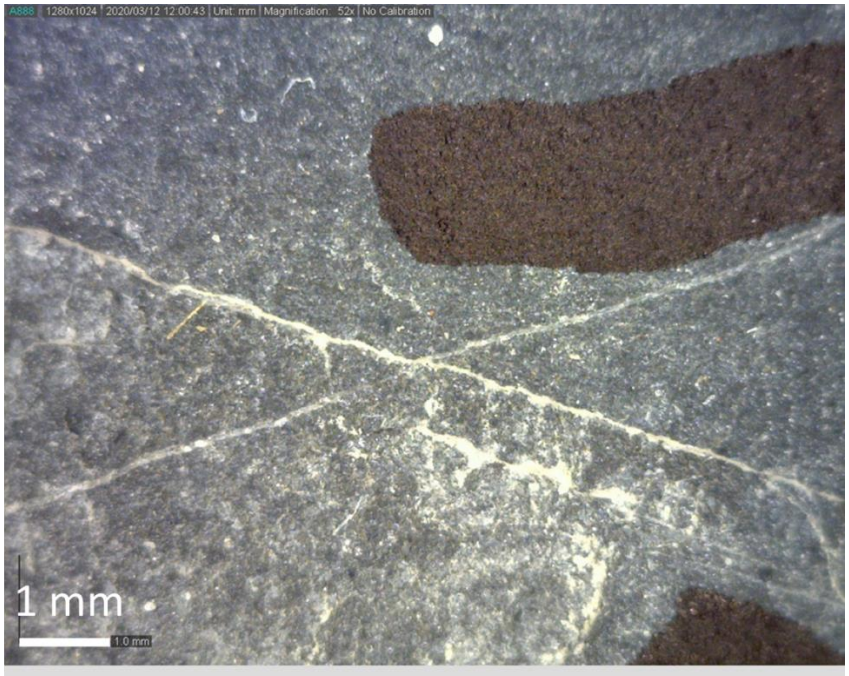

A horizontal bedding-plane exposure showing the intersection of two extension fractures in a mudstone, looking down-hole. The fractures are mineralized with calcite but the calcite has slightly different colors and crystal habits in the two fractures, indicating that they are of different ages. (The black patch at the upper right of the photo is a black line drawn on the core with a sharpie.)

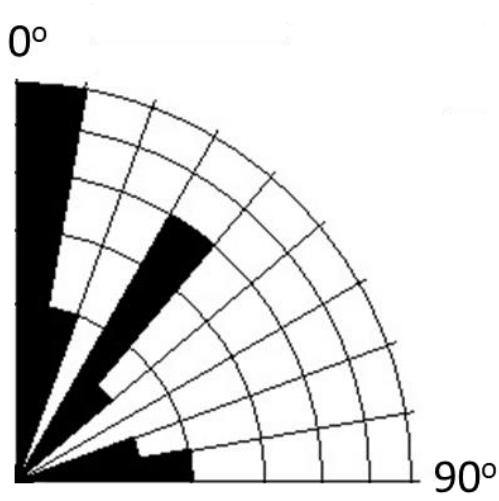

Rose plot of the measurable intersection angles between pairs of high-angle extension fractures (n = 22, min = 0°, max = 85°). Note that 0° is not north but indicates fractures of parallel strike, and 90° indicates fractures that are orthogonal to each other. The simplest (but not the only) explanation for this plot is that there are three sets of extension fractures, an interpretation which is supported by the following rose plot.

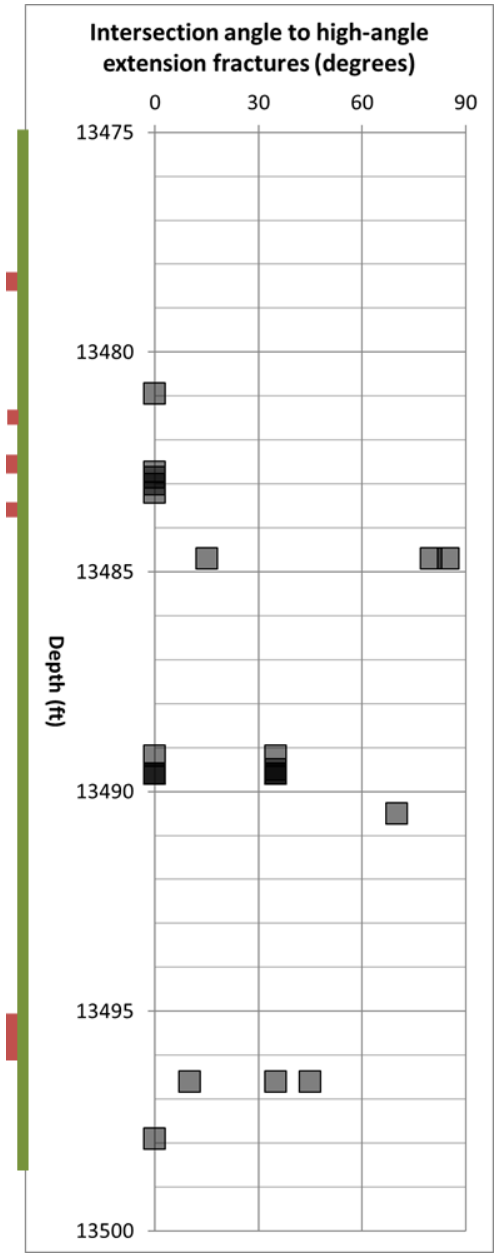

Vertical distribution of the measurable intersection angles between pairs of high-angle extension fractures (n = 126, min = 0°, max = 85°). Note 0° is not north but indicates fractures of parallel strike, 90° indicates fractures that are orthogonal to each other. This chart shows that the fracture sets with different strikes are widely distributed along the length of the core.

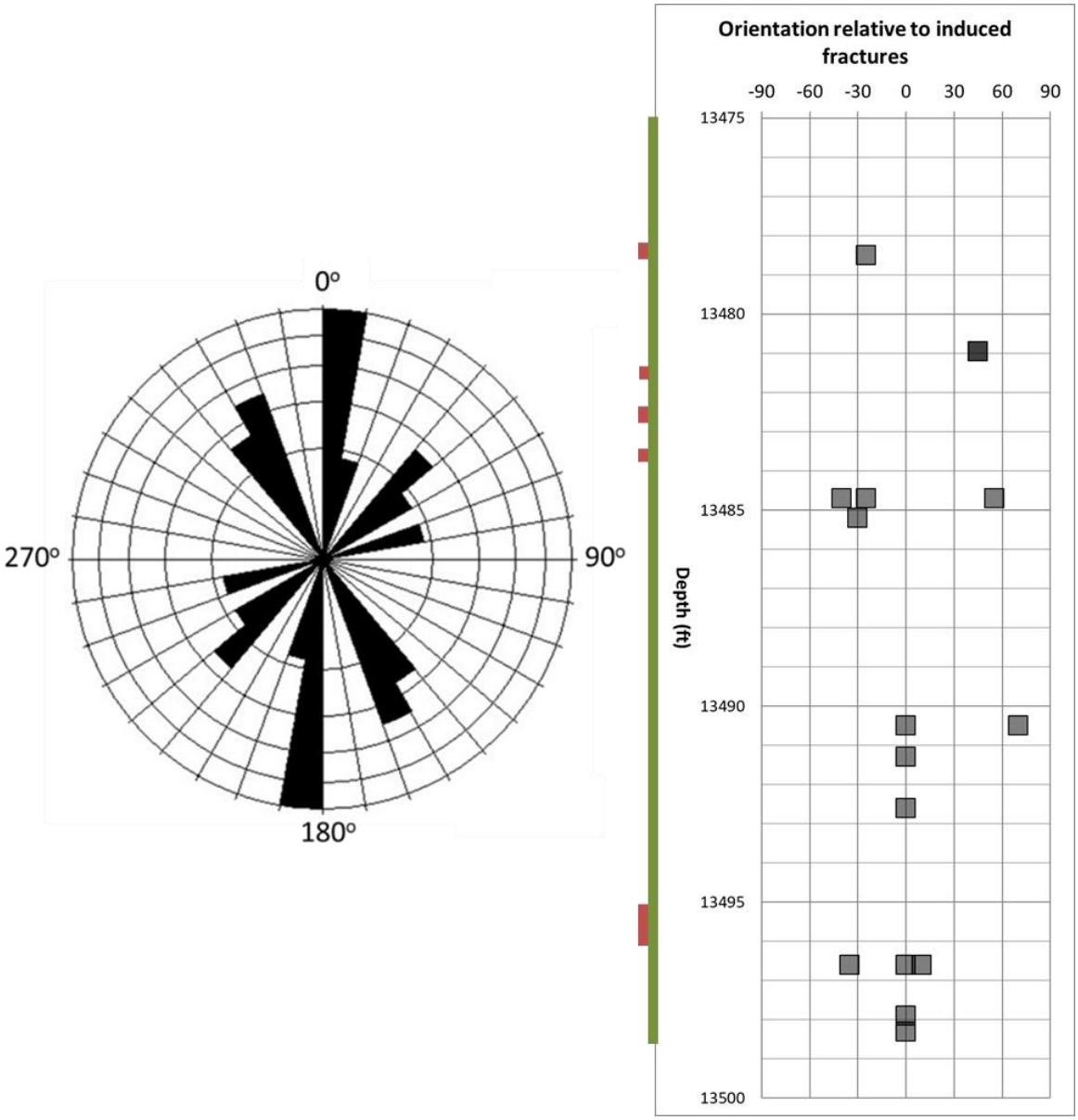

Left; the rose plot of high-angle extension fracture strikes relative to the strikes of drilling-induced petal fractures, which are plotted as the 0° reference (n = 16). The natural fractures are plotted on this rose in terms of their strike in degrees clockwise relative to the 0° reference provided by a nearby petal fracture in the core, with the maximum being 335°. The rose plot supports the inference that three fracture sets were captured by the core. Right; the depth distribution of the strikes of high-angle extension fractures relative to the strikes of drilling-induced petal fractures (n = 16, min = 0°, max = 335°). Note, 0° is not north but indicates that the natural fracture strikes parallel to a petal fracture. Minus 90° is the counterclockwise direction and plus 90° is the clockwise direction.

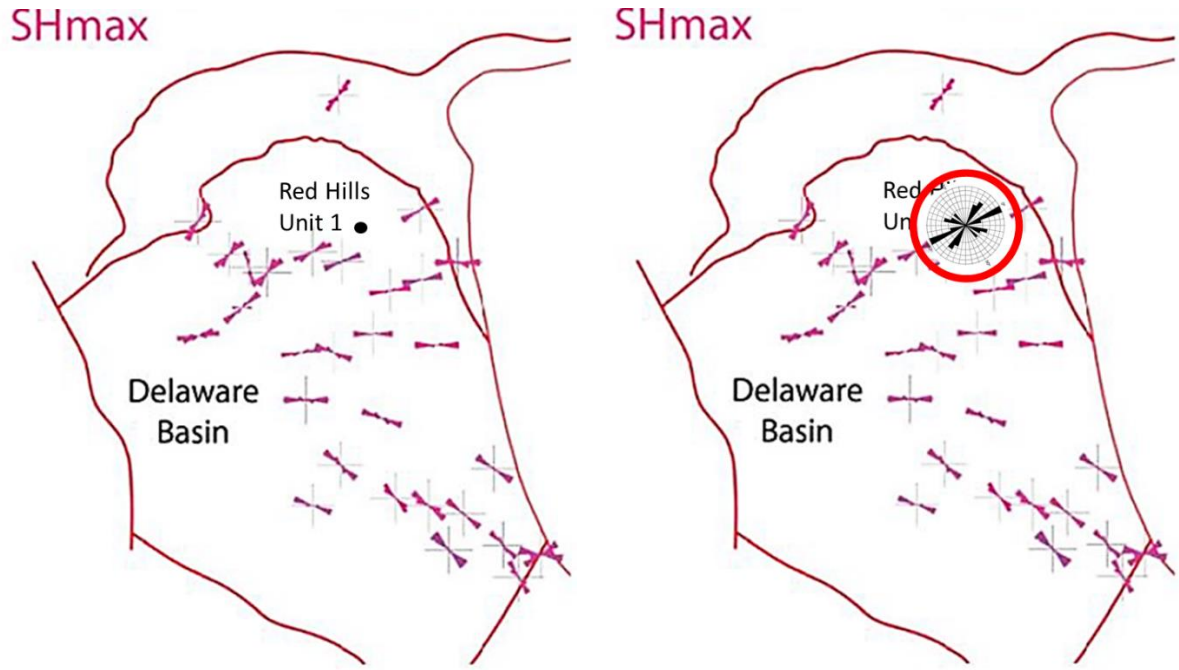

Left; orientations of the maximum horizontal compressive stress in the Delaware Basin (taken from Forand et al., 2017). The Red Hills Unit No. 1 well is in the northeastern part of the basin where the maximum horizontal compressive stress trends approximately ENE-WSW. Petal fractures in the core therefore should strike ENE-WSW, and natural fractures in the core that can be measured relative to petal fractures (the rose plot in the preceding figure) can be plotted on the map and rotated so that the petal fractures strike ENE-WSW, thus orienting the natural fractures relative to north.

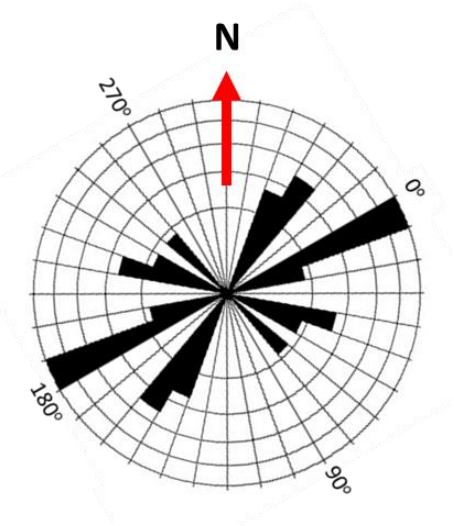

Rose plot of the strikes of natural high-angle extension fractures in the Red Hills Wolfcamp core, rotated so that the petal fractures strike parallel to the reported local maximum horizontal in situ compressive stress, suggesting that the three fracture sets strike approximately ENE-WSW (parallel to the petal fractures), NNE-SSW (20-40° counterclockwise from the petal fractures), and NW-SE (40-60° clockwise from the petal fractures).

HIGH-ANGLE SHEAR FRACTURES

One shear fracture was captured by the Red Hills core. It is poorly mineralized and probably relatively tall, so its importance is greater than the single data point would suggest. The kinematic indicators on the fracture face (steps and horizontal slickenlines), indicate right-lateral, horizontal offset.

Shear fractures in general have the potential to intersect each other as conjugate pairs, as well as to intersect the numerous vertical extension fractures in the system, thus connecting the fractured limestone layers vertically across the intervening, poorly-fractured muddy layers. Shear fractures rarely occur in isolation so other shear fractures are certain to be present in the Wolfcamp reservoir outside of the cored interval.

The small dataset for shear fractures does not support the same level of analysis that was presented for the high-angle extension fractures, and most of the characteristics are presented descriptively, with few charts and graphs. Nevertheless, the recognition that this is a different type of fracture, along with the characteristics that can be measured, provide the basis for making inferences as to the impact this fracture type has on reservoir permeability.

High-angle shear fracture; summary chart of select measured properties

Fracture type		Fractures (#)	Height (ft)	Width (mm)	Porosity %	Spacing (mm)	Dip angle (°)
shear: high-angle	Sum		0.65	0.30			
	Count	1	1	1	1		1
	Min		0.65	0.30	40		75
	Max		0.65	0.30	40		75
	Average		0.65	0.30	40.0		75.0

High-angle shear fracture ratios: number of fractures per foot of core (intensity) and average fracture height per core length (density)

Fracture type	Analysis	Fractures (#)	Fractures (%)	Sum of fracture height (ft)
shear: high-angle		1	2	0.65
Total number of fractures	1			
Total feet of fracture height	0.65			
Core interval (ft)	21.40			
Fractures (#)/cored interval (ft)	0.05			
Fracture height (ft)/cored interval (ft)	0.03			

Two views of the single inclined shear fracture captured by the Red Hills core. This fracture is hosted by a coarse-grained calcarenite limestone, and is characterized by steps and sub-horizontal slickenlines (right) which record horizontal shear. The light bar of a flashlight at the bottom of the right photo throws oblique light on the low-relief kinematic features. Shear fractures are typically interconnected: where they are poorly mineralized like this one, they are significant contributors to the reservoir fracture-permeability system.

Dip and Distribution: Shear Fracture

The cored shear fracture has a dip angle of 75°, and is hosted by a coarse-grained limestone. Since inclined fractures have a much greater probability of being intersected by a vertical core than do vertical fractures, the fact that only one was captured by the Red Hills core suggests that this fracture system is not nearly as well developed numerically as that of the high-angle extension fractures. However, since the fracture is not fully mineralized and since shear fractures have the potential to be vertically extensive, even a small number of such fractures would contribute significantly to the interconnectivity and fluid-flow potential of the Wolfcamp fracture network.

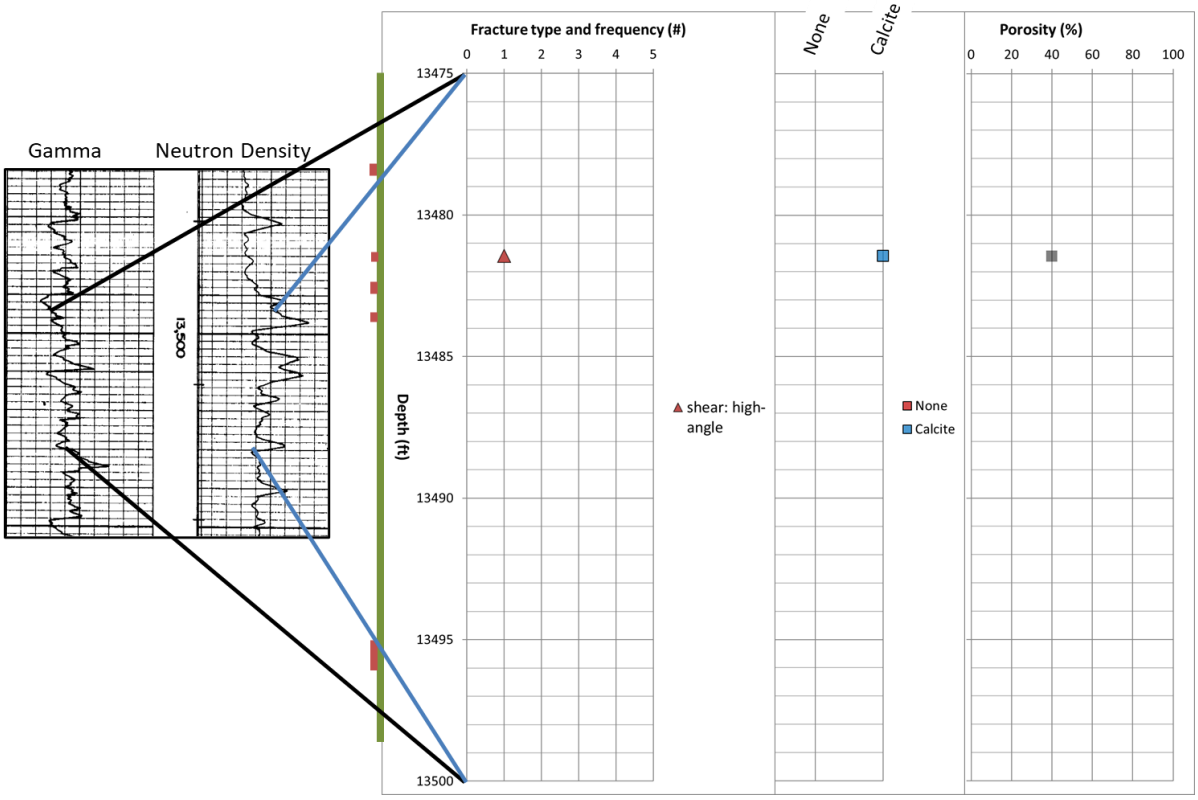

Well log, high-angle shear fracture location, mineralization, and remnant fracture porosity (n = 1).

Height and Terminations: Shear Fracture

The shear-fracture plane is inclined relative to the core axis, therefore the fracture height captured by the core (0.65 ft) is necessarily truncated and incomplete. One of the two fracture terminations is unknown because the fracture exited the side of the core before terminating, and one is blind within an apparently homogeneous lithology.

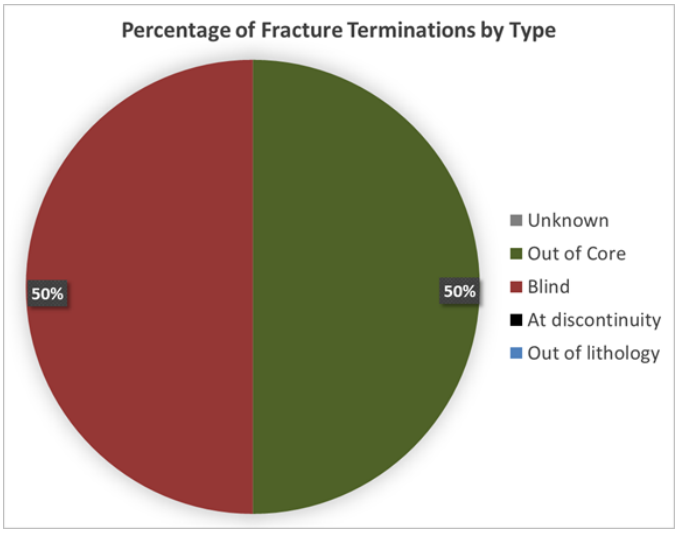

High-angle shear fracture termination chart (n = 2).

Width, Aperture, and Mineralization: Shear Fracture

The shear fracture is estimated to be 0.20 mm wide, with 40% of that width remaining as remnant fracture porosity within the calcite mineralization.

Spacing: Shear Fracture

The presence of only a single shear fracture in the core suggests that the overall spacing of these fractures is large compared to the centimeter-scale spacings of the extension fractures. Actual spacing cannot be measured in a sample population of one, but given the 15° intersection angle of the fracture plane with the axis of the core, and the lengths of core that contain no shear fractures above (6.5 ft) and below (16.5 ft) the shear plane, shear fractures must have spacings

normal to the fracture planes greater than two to five feet. Nevertheless, their height, relatively low degree of occlusion, and ability cross multiple lithologies makes them potentially important to the permeability system.

Strike: Shear Fracture

The shear fracture strikes parallel to a nearby high-angle extension fracture, but the absolute strike cannot be determined because the shear plane does not occur in a core piece that contains a petal-fracture orientation reference. Thus, the true strike of the shear fracture is unknown, and it is not apparent which of the three extension-fracture sets the shear fracture strikes parallel to.

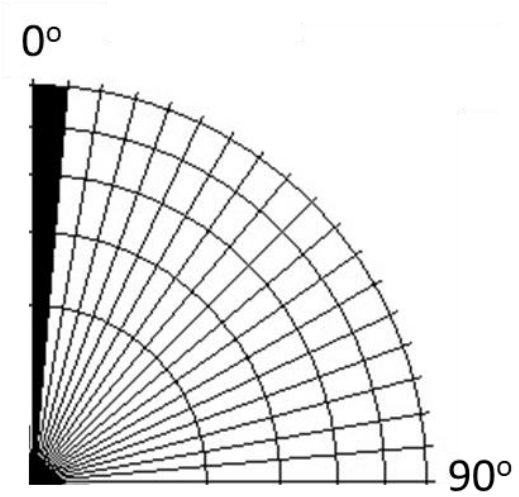

Rose plot showing the high-angle extension fracture to high-angle shear fracture intersection angle (n = 1, min = 0°, max = 0°). Note 0° is not north but indicates fractures of parallel strike.

PTYGMATICALLY-FOLDED FRACTURES

Seven small, occluded, ptygmatically-folded extension fractures also occur in the Red Hills core. This fracture type is less well developed here than in other Wolfcamp cores we have logged. Ptygmatically-folded fractures form prior to final compaction and lithification of the strata, becoming vertically shortened by folding during compaction (see Lorenz and Cooper, 2018). These few, small, isolated fractures contribute little if anything to either volume or permeability of the Wolfcamp reservoir in this well.

Ptygmatic extension fractures: summary chart of select measured properties

Fracture type		Fractures (#)	Height (ft)	Width (mm)	Porosity %	Spacing (mm)	Dip angle (°)
extension: ptygmatic	**Sum**		0.12	0.65			
	Count	7	7	7	7		7
	Min		0.01	0.05	0		80
	Max		0.02	0.10	0		90
	Average		0.02	0.09	0.0		87.9

Ptygmatic extension fractures: ratios of number per foot of core (intensity) and fracture height per core height (density)

Fracture type	Analysis	Fractures (#)	Fractures (%)	Sum of fracture height (ft)
extension: ptygmatic		7	14	0.12
Total number of fractures	7			
Total feet of fracture height	0.12			
Core interval (ft)	21.40			
Fractures (#)/cored interval (ft)	0.33			
Fracture height (ft)/cored interval (ft)	0.01			

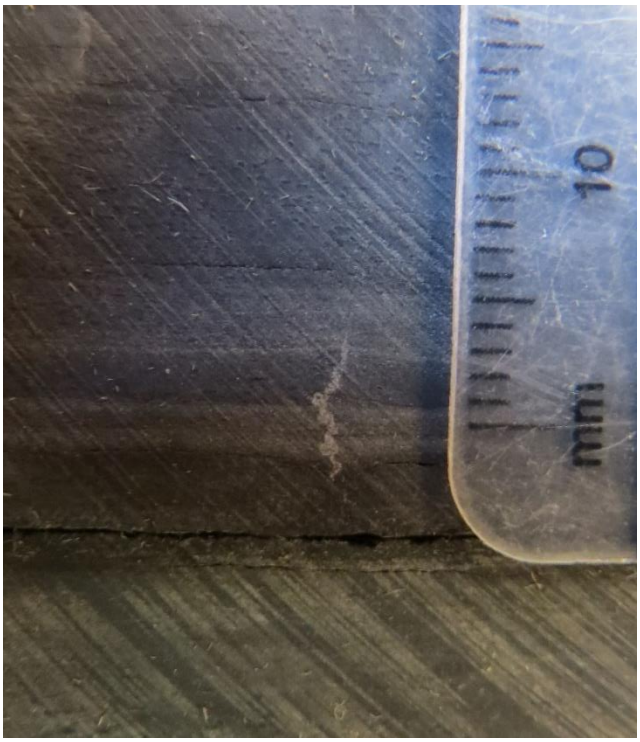

A short, ptygmatically-folded fracture in a laminated mudstone and limestone facies. These fractures are occluded by mineralization and are not vertically extensive, therefore they contribute little to reservoir permeability. The diagonal fabric marking the slab face, sweeping from upper left to lower right, is an artifact, a pattern created by the rock saw during slabbing.

Dips and Distributions: Ptygmatically-Folded Fractures

The ptygmatically-folded fractures are vertical, and they are concentrated in the upper, somewhat muddier section of the Red Hills core. Five fractures occur in an interbedded mudstone-limestone facies, and two occur in more homogeneous mudstones: none formed in either of the two limestone facies.

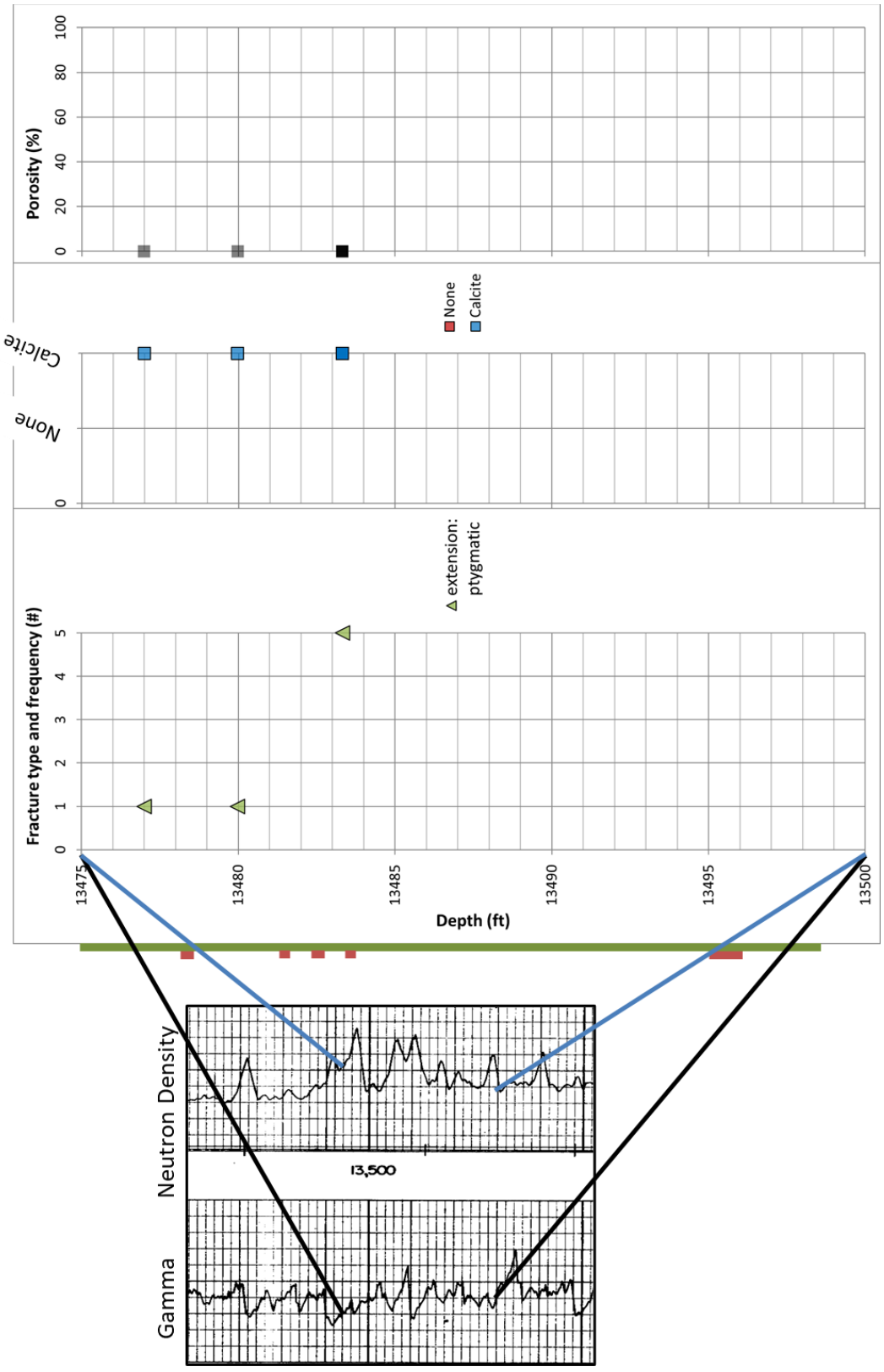

Ptygmatically-folded extension fractures; well logs, vertical distribution, fracture fill components, and average remnant porosity, by depth (n = 7).

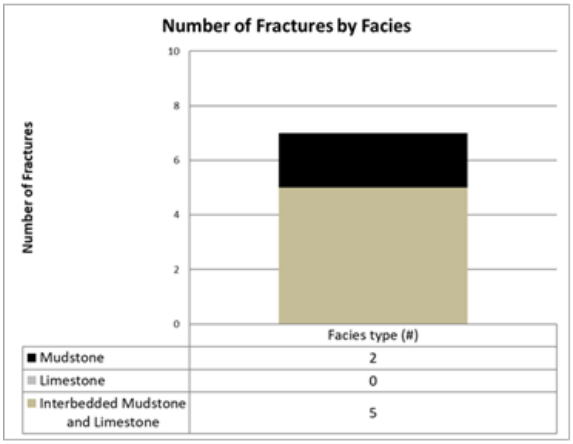

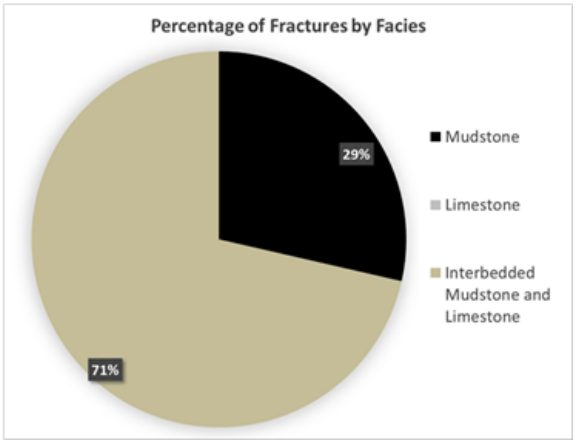

Ptygmatic extension fractures related to the lithologic facies that contains the majority of their height (n = 7). Fractures within facies percentages: mudstone (28.6%), limestone (0%), interbedded mudstone and limestone (71.4%).

Heights and Terminations: Ptygmatically-Folded Fractures

The ptygmatically-folded extension fractures are short, averaging only 0.017 ft (5 mm) tall, and both top and bottom terminations of all fractures are present in the core: none of the heights are truncated. All fractures terminate just outside of the bed that hosts them, thus all fractures are approximately as tall as the thickness of their host beds.

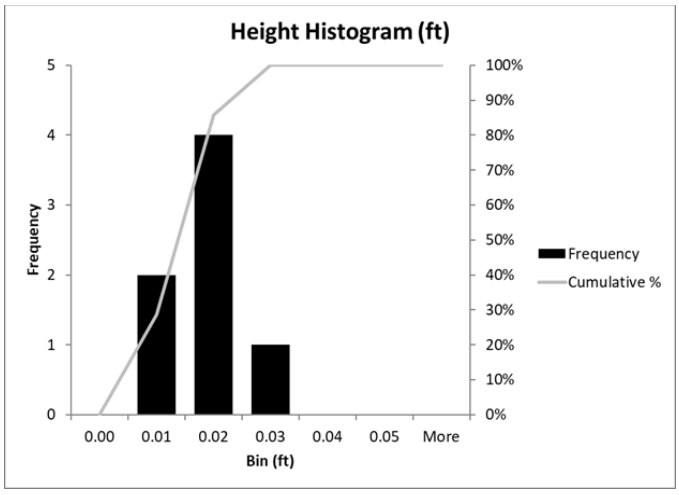

Ptygmatic extension fracture height histogram (n = 7; min 0.01, max 0.02, ave 0.017 ft).

Widths, Aperture, and Mineralization: Ptygmatically-Folded Fractures

Ptygmatically-folded extension fractures are narrow, averaging slightly less than a tenth of a millimeter wide, and they are 100 percent occluded by calcite.

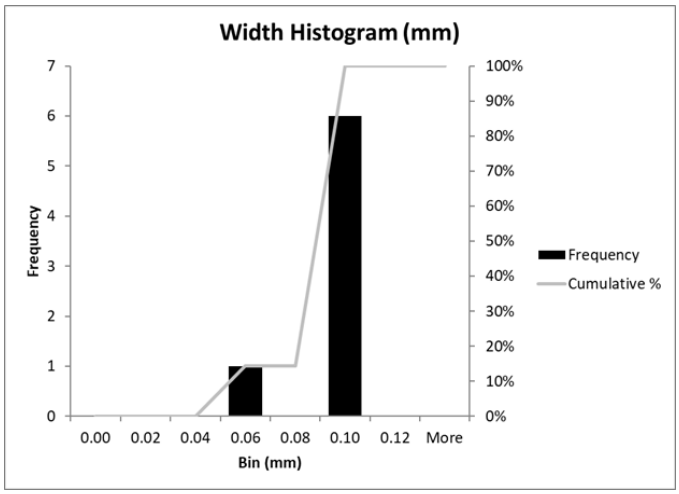

Ptygmatic extension fracture width histogram (n = 7; min 0.05, max 0.10, ave 0.09 mm).

Spacing and Strike: Ptygmatically-Folded Fractures

These small fractures are difficult to trace from one side of the core to another, therefore their strikes and spacings cannot be determined without breaking or cutting the core to expose a view in the horizontal plane.

EFFECTIVENESS OF THE WOLFCAMP NATURAL-FRACTURE SYSTEM

FRACTURE vs. MATRIX POROSITY AND PERMEABILITY

The available well records from the Red Hills Unit No. 1 well make no reference to the numerous natural fractures we logged in this core: the fractures were probably considered to be too small to be significant at a time, in the early 1960s, when drilling targets were high-porosity/high-permeability conventional reservoirs. The records note that the core had "no [matrix] porosity, and no shows". However, the records also describe a Wolfcamp drill-stem test and indications of lost circulation in the tested interval, both signifying that the Wolfcamp reservoir is not impermeable. From the well records:

> *"[Drill-Stem] Tool open 6 hrs 24 minutes, attempted to flow through separator, would not work. Flowed to pit, stabilized pressure 1700# at 12 MMCF/D. Opened by-pass on test tool, circulated, lost 650 barrels mud, pulled tool….Reamed core hole 13,4750-13,499. Drilled 13,499-13,612, started losing mud, lost complete returns."*

Despite the apparent absence of matrix porosity in the core, the Wolfcamp reservoir as a whole does contain porosity and interconnected permeability that are significant in an unconventional reservoir. Fluid flow from, and lost circulation within, a zone of low matrix permeabilities can be accounted for by a pervasive system of natural fractures in the reservoir. The presence of so many fractures in the 21.4 ft of core accounts for both the lost circulation and the high flow capacity from what appeared to be poor-quality reservoir rock, and the core shows that the Wolfcamp reservoir is laced with a pervasive system of numerous, albeit relatively small, natural factures. The Wolfcamp Formation in the Red Hills well might be capable of producing un-stimulated provided that the fracture-permeability system remains un-damaged by drilling fluids and cementing operations.

The reservoir is also significantly overpressured: the reported Instantaneous Shut-In Pressure (ISP) of 11,400 psi at this depth indicates a pressure gradient of about 0.8 psi/ft. These narrow fractures may be stress-sensitive, and if so they would close down as fluid pressure was withdrawn from the fracture apertures during production.

FRACTURE VOLUMETRICS

The measured fracture widths, heights, and remnant fracture porosities, along with the core diameter, can be used to estimate an effective volume for each individual fracture, and to calculate an average effective volume for each of the three fracture types. The effective volumes can then be used to estimate the relative effective permeabilities of the three fracture types. As shown by the following tables, the ptygmatically-folded extension fractures offer no contribution to the reservoir. In contrast, both high-angle extension fractures and high-angle shear fractures provide significant potential for enhanced permeability, well above what are probably nanodarcy-scale matrix permeabilities.

Significantly, the calculations (best used as relative numbers for comparisons, and used only with caution as absolute numbers for modeling parameters) show that *per fracture,* shear fractures offer about ten times more volume than extension fractures, and, because they are significantly wider, probably well over ten times more permeability. Moreover, the total fracture volume provided by the single shear fracture is over twice that provided by the entire population of 42 extension fractures combined, since the shear fracture is so much wider and less occluded by mineralization.

Shear fractures therefore have the potential to be very important. Add this to the potential for these fractures to extend across bedding, and to interconnect with each other and the extension fractures, and it becomes apparent that shear fractures probably form a vital part of the reservoir plumbing system. Shear fractures provide fluid-flow highways to the wellbore, being fed by the pervasive system of numerous narrow, vertically-limited extension fractures.

A hydraulic stimulation fracture imposed onto this system would have an effect similar to that of the shear fractures, connecting the smaller extension fractures and potentially breaking up the matrix rock with additional induced fractures. A cautionary note: narrow extension fractures have a high probability of being damaged by 1) the additional stresses superimposed onto the system by wide, propped injections, which would preferentially close those ENE-WSW trending natural fractures oriented parallel to the in situ maximum horizontal compressive stress, and by 2) capillary forces associated with injection fluids, which would act to close the narrow fracture apertures. Moreover, the other two extension-fracture sets, trending NNE-SSW, and NW-SE,

oblique to the in situ stress axes, would be subjected to shear as the in situ stress magnitudes change during production; a little shear offset, a few millimeters or less, would open fracture apertures and enhance fracture permeability, but continued shear would quickly fill the fractures with gouge and reduce fracture permeability. Nevertheless, this reservoir has the potential to be productive if completed and produced judiciously. The well could conceivably produce without being stimulated, likely at a relatively low rate but with a shallow decline curve.

High-angle extension fracture effectiveness: General summary of select measured properties used to calculate 1) effective aperture, 2) fracture volume, and 3) effective volume

Fracture type		# Fractures	Fracture vertical height (ft)	Average fracture width (mm)	Remnant fracture porosity (%)	Effective aperture (mm)	Fracture volume (mm^3)	Effective Fracture volume (mm^3)
extension: high-angle	Sum		10.60	6.55		1	76379	10517
	Count	42	42	42	42	42	42	42
	Min		0.03	0.05	0	0.00	51	0
	Max		1.65	0.40	90	0.12	16766	2845
	Average		0.25	0.16	10.8	0.0208	1819	250

High-angle shear fracture effectiveness: General summary of select measured properties used to calculate effective aperture, fracture volume, and effective volume

Fracture type		# Fractures	Fracture vertical height (ft)	Average fracture width (mm)	Remnant fracture porosity (%)	Effective aperture (mm)	Fracture volume (mm^3)	Effective Fracture volume (mm^3)
shear: high-angle	Sum		0.65	0.30		0.12	6605	2642
	Count	1	1	1	1	1	1	1
	Min		0.65	0.30	40	0.12	6605	2642
	Max		0.65	0.30	40	0.12	6605	2642
	Average		0.65	0.30	40.0	0.1200	6605	2642

High-angle, ptygmatically-folded extension fracture effectiveness: General summary of select measured properties used to calculate effective aperture, fracture volume, and effective volume

Fracture type		# Fractures	Fracture vertical height (ft)	Average fracture width (mm)	Remnant fracture porosity (%)	Effective aperture (mm)	Fracture volume (mm^3)	Effective Fracture volume (mm^3)
extension: prtygmatic	Sum		0.12	0.65		0.00	344	0
	Count	7	7	7	7	7	7	7
	Min		0.01	0.05	0	0.00	31	0
	Max		0.02	0.10	0	0.00	62	0
	Average		0.02	0.09	0.0	0.0000	49	0

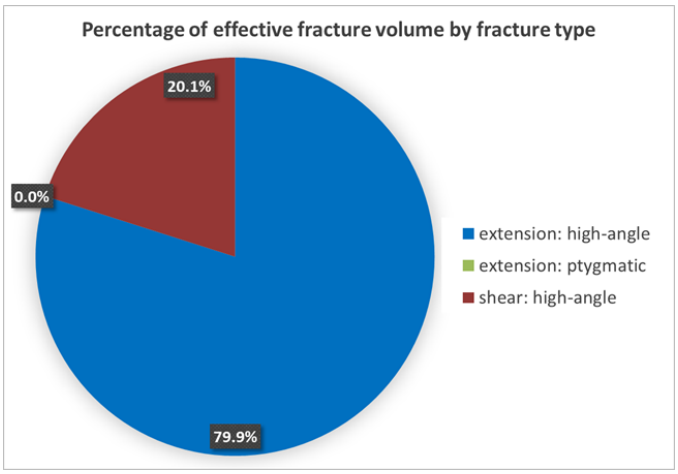

Summary of total percentage of effective fracture volume by fracture type. This chart shows: 1) ptygmatically-folded fractures have no effective volume, 2) the single, high-angle shear makes up 20.1% of the total effective volume and 3) the 42 high-angle extension fractures encompass the remaining 79.9% of the total effective fracture volume (effective fracture volume = fracture volume x remnant porosity).

CONCLUSIONS

The fracture-permeability system in the Wolfcamp Formation, as documented by a population of 50 natural fractures in 21.4 ft of core, is comprised of three fracture types. Whereas the sub-population of seven small, occluded, high-angle, ptygmatically-folded extension fractures contributes nothing to the permeability system, two other sub-populations of 42 high-angle extension fractures and one shear fracture together form an important, interconnected permeability network. The numerous narrow, incompletely-mineralized, and intersecting extension fractures form hydraulically-linked networks within the limestone beds, but provide little or no vertical communication across the interbedded mudstones. The extension fractures strike ENE-WSW, NNE-SSW, and NW-SE, and are very closely spaced. Fewer, wider, and less-mineralized shear fractures connect the bedding-bound networks, providing vertical connectivity and localized high-permeability fluid-flow pathways. A drill-stem test and lost circulation show that this natural-fracture network significantly enhances system permeability over matrix values, such that the Wolfcamp reservoir may be able to produce, albeit at relatively low rates, without being hydraulically fractured. A hydraulic stimulation would enhance the production rate, provided little or no damage is done to the natural-fracture permeability network.

CITED REFERENCES

Core Laboratories Inc., 1982 [December], Core fracture study, No. 1 Robert L. Todd et al., West Feliciana Parish, Louisiana; 45 pages (provided by Marathon Oil Company).

Finley, S.J., and Lorenz, J.C., 1988, Characterization of natural fractures in Mesaverde core from the Multiwell Experiment, Sandia National Laboratories Technical Report, SAND88-1800, 133p.

Finley, S.J., and Lorenz, J.C., 1989, Characterization and significance of natural fractures in Mesaverde reservoirs at the Multiwell Experiment site: SPE 19007, in Proceedings of the Soc. Petrol Engineers Rocky Mountain Regional Symposium, Denver, CO, p. 721-728.

Forand, D., Heesakkers, V., & Schwartz, K., 2017, Constraints on Natural Fracture and In-situ Stress Trends of Unconventional Reservoirs in the Permian Basin, USA. Unconventional Resources Technology Conference. doi:10.15530/URTEC-2017-2669208.

Kvale, E.P., Bowie, C.M., Flenthrope, C., Mace, C., Parrish, J.M., Price, B., Anderson, S., and DiMichele, W.A., 2020, Facies variability within a mixed carbonate–siliciclastic sea-floor fan (upper Wolfcamp Formation, Permian, Delaware Basin, New Mexico); AAPG Bulletin, v. 104, pp. 525–563.

Lorenz, J.C., Finley, S.J., and Warpinski, N.R., 1990, Significance of coring-induced fractures in Mesaverde core, northwestern Colorado: American Association of Petroleum Geologists Bulletin, v. 74, p. 1017-1029.

Lorenz, J.C., and Hill, R.E., 1992, Measurement and analysis of fractures in core, in, J.W. Schmoker, E. B. Coalson, C. A. Brown, Editors, Geological Studies Relevant to Horizontal Drilling: Examples from Western North America: Rocky Mountain Association of Geologists, p. 47-59.

Lorenz, J.C., and Cooper, S.P., 2018, Atlas of Natural and Induced Fractures in Core; Wiley and Sons, 315 pages.

Lorenz, J.C., and Cooper, S.P., 2020, Applied Concepts in Fractured Reservoirs; Wiley and Sons, 211 p.

Nelson, R.A., 2002, Geologic Analysis of Naturally Fractured Reservoirs, /2nd edition, Gulf Professional Publishing. Boston, 332 p.

Thompson, Michelle & Desjardins, Patricio & Pickering, Jennifer & Driskill, Brian, 2018, An Integrated View of the Petrology, Sedimentology, and Sequence Stratigraphy of the Wolfcamp Formation, Delaware Basin, Texas. 10.15530/urtec-2018-2901513. https://www.researchgate.net/figure/Stratigraphic-nomenclature-for-the-Wolfcamp-Formation-in-the-Delaware-Basin-IHS-2017_fig1_326607198 Accessed March 20, 2020

APPENDIX A
Definitions

This report uses the following terminology, adapted from Lorenz and Cooper (2018), for measuring and reporting fracture parameters:

Fracture width: The distance between the host-rock walls, not including any mineralization. Width is measured in millimeters. The space between fracture walls controls permeability, but that space may be partially or completely occluded by mineralization. A facture may be completely occluded by mineralization but still have width. Widths may vary along a fracture length and height, especially for shear fractures. Extension fractures have more uniform widths but they typically narrow at the upper and lower terminations. The widths reported here are the average widths along fractures.

Fracture aperture: The dimension of the open void space in a fracture measured normal to the fracture walls is its aperture, also measured in millimeters. If the fracture is un-mineralized, then its aperture is equal to its width. If the fracture is completely filled by mineralization, then it has width but no aperture. It is often difficult to characterize fracture apertures in terms of a linear dimension since many fractures, especially shear fractures, and extension fractures that are partially mineralized or subjected to dissolution, have irregular apertures. Apertures in fractures with crystalline mineralization commonly resemble the irregular open void spaces between clenched teeth, between which fluid will flow but which cannot realistically be characterized by a single number of millimeters. Thus, we have also estimated remnant fracture porosity (see next).

Remnant fracture porosity: The open void space within a fracture, measured in percent of the original width that is not occluded by mineralization. It is estimated visually by comparison to charts of known percentages. An un-mineralized fracture retains 100% of its original width as void space (i.e., '100% remnant fracture porosity') regardless of its width. A fracture that has been completely occluded by mineralization or clay fill has 0% remnant fracture porosity.

Bulk fracture porosity: The contribution of fracture void space to the total/bulk volume of the rock, measured in percent. Even in highly fractured reservoirs this is typically less than 1% and rarely approaches 2% (e.g., Nelson, 2002).

Effective fractures: An effective fracture is one that 1) has enough remnant fracture porosity to be a conduit to fluid flow and enhance permeability above matrix values, and that 2) is an interconnected part of the fracture-permeability system. An isolated short, wide, and open fracture can be an individual high-permeability conduit but it is not effective because that permeability leads nowhere.

Fracture facies: A suite of one or more fracture types and intensities that is characteristic of one geomechanical, stratigraphic, or lithologic unit.

Fracture intensity: A measure of the degree of fracture development calculated as the number of fractures per core length (the "P_{10}" of some usages), and sometimes restricted to the number of fractures per foot of fracture-prone lithology in the core.

Fracture density: A measure of the degree of fracture development calculated as the ratio of cumulative fracture height to core length, sometimes restricted to the height of fractures per foot of fracture-prone lithology in the core.

APPENDIX B

Methods

Logging

During the core logging for this report, the core pieces were removed from the boxes and examined carefully on all surfaces using the methods outlined by Lorenz and Hill (1992) in order to find all of the cored fractures. Core butts comprise some 75-80% of the sample volume provided by a core and commonly contain fractures that do not intersect either the slab face or any part of the slabs, thus the absence of the slabs for the Red Hills core did not significantly degrade the fracture population obtained from this core.

The narrowest fractures are difficult to see on the rough, external core surfaces, so a minor percentage of smaller fractures that did not intersect the slab face may have been missed. Where possible and practical, the core pieces were re-assembled and locked end-to-end to determine the relative strikes of two or more fractures. The cores and fractures were photographed, and the photos are included in a database that was constructed for this report. The characteristics of each fracture were recorded and logged in an Excel file. The Table of Contents for this database is provided in Appendix C, and the database itself can be requested from FractureStudies LLC (see www.fractures.com).

Fracture Strikes

Fracture strikes in a core can be assessed several ways. The simplest and easiest measurements are of fracture strikes relative to each other, possible where two fractures occur in the same piece of core or where two fractures occur in different core pieces that can be locked together.

Many fracture pairs are parallel, having a measured “intersection” angle of 0°, which suggests anisotropic fracture-controlled drainage. However, two measurements of parallel fractures, when obtained from different, non-contiguous sections of core, are not necessarily indicate that all fractures belong to the same set of parallel fractures, and may in fact represent two fracture sets unless the data are further constrained by an independent orientation reference.

Fracture pairs that have oblique or even right-angle strikes indicate the presence of an interconnected fracture network and suggest more isotropic drainage.

Many fracture strikes in the Red Hills core could also be referenced to the common induced petal fractures which consistently strike parallel to the maximum horizontal in situ compressive stress (see Lorenz et al., 1990). Since the trend of the in situ stress relative to north is known, the natural and petal fracture strikes can be rotated and oriented relative to north.

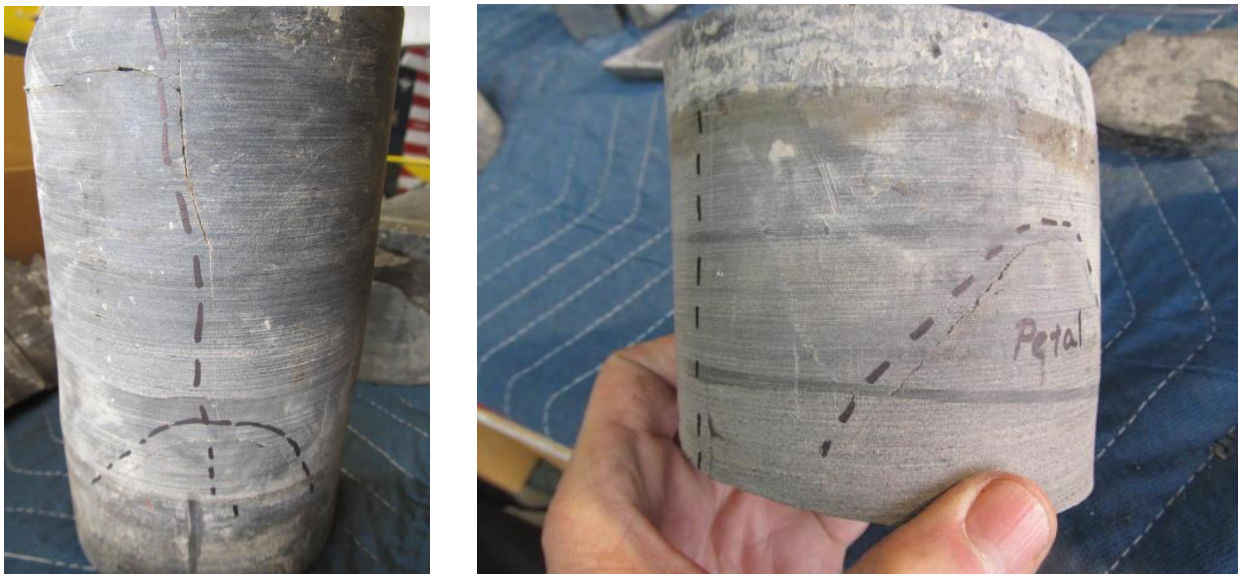

Petal fractures (the rainbow arcs outlined by dashed sharpie lines drawn on the core) are created at the bottom of the hole during coring, and consistently strike parallel to the maximum horizontal in situ compressive stress. Petal fractures therefore provide an orientation reference in the core. The vertical extension fractures (also marked by vertical dashed sharpie lines) in these core pieces strike nearly normal (left) and oblique (right) to the petal fractures, therefore the two pictured extension fractures can be determined to be oblique to each other even though the two pieces come from different parts of the core that cannot be locked together.

Quantitative and Semi-Quantitative Data

Many fractures are well-exposed, discrete structures that are easy to measure, and for these we have measured exact widths, heights, strikes, etc. However, of necessity some of the data presented in this report are semi-quantitative; i.e., although we have provided discrete numbers for the various fracture parameters, those numbers are best estimates, based on context,

experience, and locally on the resemblance of an obscure fracture to similar, better-exposed fractures in other parts of the core. No data are entered for fracture parameters that could not be measured or estimated, for example ‘strike’ where a fracture was exposed on only one core surface, and where parameters like height and width could be measured but strike is unconstrained.

Some of the reported height measurements are minima because the full fracture height is unknown, i.e., fractures may exit the sides of the core upward and downward before terminating, or the terminations may be lost in missing core or rubble zones. Such minima are useful, providing lower boundaries on fracture heights.

APPENDIX C

Table of Contents for Worksheets in the Full Excel Database

Red Hills #1: Core Database

1. Cover sheet
2. Fracture types and abbreviations
3. Core data sheet
4. Short summary
5. Full summary
6. All core datasheet
    a. Extension: high-angle
    b. Extension: ptygmatic
    c. Shear: high-angle
7. Fracture type by depth
8. Dip-angle by depth
    a. Dip-angle histogram
9. Fracture fill/mineralization
10. Fracture porosity etc. by depth
11. Fracture
    a. Terminations
    b. Truncations
12. Fracture density by depth
13. Fracture lithology by depth
14. Fracture width, height, aperture, volume by depth
15. Effectiveness charts
16. Extension fractures: high-angle
    a. Fill/mineralization
    b. Porosity, height etc.
    c. Terminations
    d. Truncations
    e. Lithology
    f. Width, height, effectiveness etc.
    g. Height histogram
    h. Width histogram
    i. Dip-angle histogram
    j. Porosity histogram
    k. Spacing histogram
    l. Orientation
17. Extension fractures: ptygmatic
    a. Fill/mineralization
    b. Porosity, height etc.
    c. Terminations
    d. Truncations
    e. Lithology

    f. Width, height, effectiveness etc.
    g. Height histogram
    h. Width histogram
    i. Dip-angle histogram
    j. Porosity histogram
18. Shear fractures: high-angle
    a. Fill/mineralization
    b. Porosity, height etc.
    c. Terminations
    d. Truncations
    e. Lithology
    f. Height histogram
    g. Width histogram
    h. Dip-angle histogram
    i. Porosity histogram

The first few Excel worksheets are provided below: